

## Electronic Supplementary Information

For

### Silver Ion-Induced Chiral Enhancement by Argentivorous Molecules

Eunji Lee,<sup>a</sup> Yasuhiro Hosoi,<sup>a</sup> Honoka Temma,<sup>a</sup> Huiyeong Ju,<sup>a</sup> Mari Ikeda,<sup>b</sup> Shunsuke Kuwahara<sup>a,c</sup> and Yoichi Habata<sup>\*a,c</sup>

<sup>a</sup>*Department of Chemistry, Faculty of Science, Toho University, 2-2-1 Miyama, Funabashi, Chiba 274-8510, Japan*

<sup>b</sup>*Education Centre, Faculty of Engineering, Chiba Institute of Technology, 2-1-1 Shibazono, Narashino, Chiba 275-0023, Japan*

<sup>c</sup>*Research Centre for Materials with Integrated Properties, Toho University, 2-2-1 Miyama, Funabashi, Chiba 274-8510, Japan*

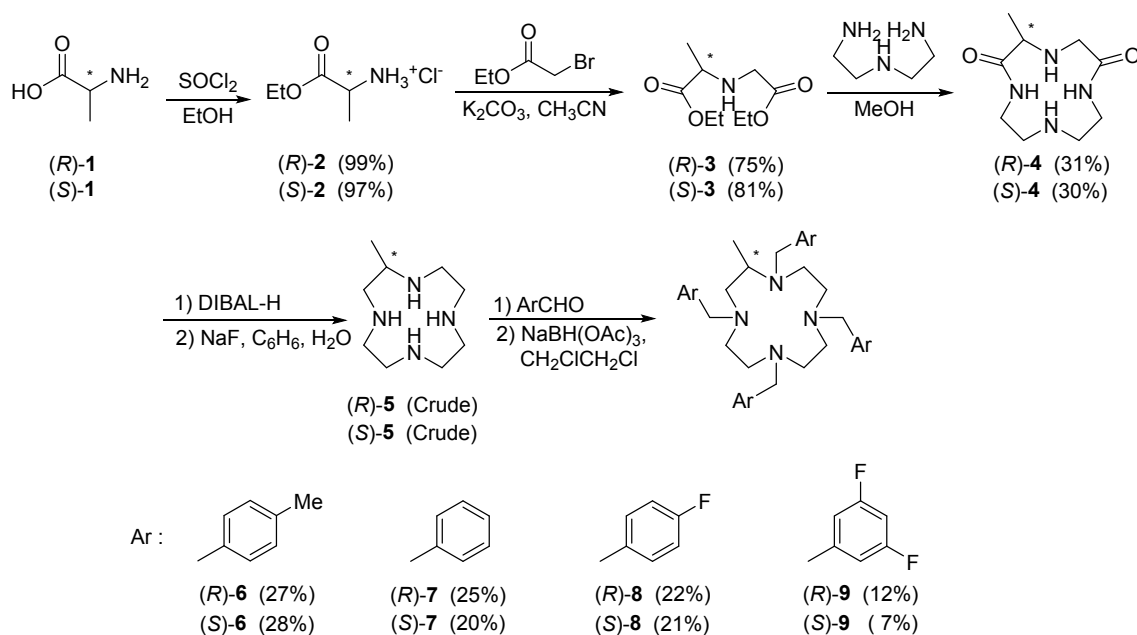
# Table of Contents

<b>Experimental Procedures</b> .....	3
<b>General</b> .....	3
<b>Synthesis of (R or S)-6-9</b> .....	3
<b>Preparation of (R)-6-AgPF<sub>6</sub></b> .....	6
<b>Preparation of (S)-6-AgPF<sub>6</sub></b> .....	6
<b>Preparation of (S)-7-AgBF<sub>4</sub></b> .....	6
<b>Preparation of (R)-8-AgPF<sub>6</sub></b> .....	6
<b>Preparation of (R)-6-Zn(NO<sub>3</sub>)<sub>2</sub></b> .....	6
<b>Results and Discussion</b> .....	7
<b>Fig. S1</b> Four isomers of metal complexes with a tetra-armed cyclen.....	7
<b>Fig. S2</b> <sup>1</sup> H and <sup>13</sup> C NMR spectra of (R)-6 .....	7
<b>Fig. S3</b> <sup>1</sup> H and <sup>13</sup> C NMR spectra of (S)-6 .....	8
<b>Fig. S4</b> <sup>1</sup> H and <sup>13</sup> C NMR spectra of (R)-7 .....	9
<b>Fig. S5</b> <sup>1</sup> H and <sup>13</sup> C NMR spectra of (S)-7 .....	10
<b>Fig. S6</b> <sup>1</sup> H and <sup>13</sup> C NMR spectra of (R)-8 .....	11
<b>Fig. S7</b> <sup>1</sup> H and <sup>13</sup> C NMR spectra of (S)-8 .....	12
<b>Fig. S8</b> <sup>1</sup> H and <sup>13</sup> C NMR spectra of (R)-9 .....	13
<b>Fig. S9</b> <sup>1</sup> H and <sup>13</sup> C NMR spectra of (S)-9 .....	14
<b>Fig. S10</b> CD spectra of (R)-7 and (S)-7 in the presence of metal triflates.....	15
<b>Fig. S11</b> CD spectra of (R)-8 and (S)-8 in the presence of metal triflates.....	15
<b>Fig. S12</b> CD spectra of (R)-9 and (S)-9 in the presence of metal triflates.....	16
<b>Fig. S13</b> CD spectral changes of (R)-7 and (S)-7 upon addition of silver(I).....	16
<b>Fig. S14</b> CD spectral changes of (R)-8 and (S)-8 upon addition of silver(I).....	17
<b>Fig. S15</b> CD spectral changes of (R)-9 and (S)-9 upon addition of silver(I).....	17
<b>Fig. S16</b> UV-Vis spectral changes of (R)-6 upon addition of silver(I) triflate .....	18
<b>Fig. S17</b> UV-Vis spectral changes of (R)-7 upon addition of silver(I) triflate .....	18
<b>Fig. S18</b> UV-Vis spectral changes of (R)-8 upon addition of silver(I) triflate .....	19
<b>Fig. S19</b> UV-Vis spectral changes of (R)-9 upon addition of silver(I) triflate .....	19
<b>Fig. S20</b> HMBC and HMQC spectra of (R)-6 with silver(I) triflate.....	20
<b>Fig. S21</b> HMBC and HMQC spectra of (R)-7 with silver(I) triflate.....	20
<b>Fig. S22</b> HMBC and HMQC spectra of (R)-8 with silver(I) triflate.....	20
<b>Fig. S23</b> HMBC and HMQC spectra of (R)-9 with silver(I) triflate.....	21
<b>Fig. S24</b> Silver(I)-induced <sup>1</sup> H NMR spectral changes of (R)-7 .....	21
<b>Fig. S25</b> Silver(I)-induced <sup>1</sup> H NMR spectral changes of (R)-8 .....	22
<b>Fig. S26</b> Silver(I)-induced <sup>1</sup> H NMR spectral changes of (R)-9 .....	22
<b>Fig. S27</b> Four isomers of Ag <sup>+</sup> complexes with a chiral tetra-armed cyclen.....	23
<b>Fig. S28</b> Molecular modeling calculation of Ag <sup>+</sup> complex of (R)-7 .....	23
<b>Table S1</b> Molecular modeling calculation of (R)-7-Ag <sup>+</sup> complex.....	23
<b>Table S2</b> Molar ellipticity and ε of the Ag <sup>+</sup> complexes with chiral cyclens and minimum of potential energy, and dipole moments .....	24
<b>Fig. S29</b> Electrostatic potential maps of substituted benzenes and Comparison of the CD spectra of each ligand with silver(I) .....	24
<b>Fig. S30</b> Ag <sup>+</sup> -induced change in optical rotation titration of each ligand with Ag <sup>+</sup> .....	25
<b>Fig. S31</b> Crystal structures of (R)-6 and (S)-6 with AgPF <sub>6</sub> .....	25
<b>Fig. S32</b> Crystal structure of (S)-7 with AgBF <sub>4</sub> .....	25
<b>Fig. S33</b> Crystal structure of (R)-8 with AgPF <sub>6</sub> .....	26
<b>Fig. S34</b> Crystal structure of (R)-6 with Zn(NO <sub>3</sub> ) <sub>2</sub> .....	26
<b>Fig. S35</b> Methyl proton signals in the Ag <sup>+</sup> /(R)-8 system.....	27
<b>X-ray crystallographic analysis</b> .....	28
<b>Table S3</b> Crystal and experimental data .....	28
<b>Table S4</b> Selected bond lengths (Å) and bond angles (°) for (R)-6-AgPF <sub>6</sub> .....	29
<b>Table S5</b> Selected bond lengths (Å) and bond angles (°) for (S)-6-AgPF <sub>6</sub> .....	29
<b>Table S6</b> Selected bond lengths (Å) and bond angles (°) for (S)-7-AgBF <sub>4</sub> .....	29
<b>Table S7</b> Selected bond lengths (Å) and bond angles (°) for (R)-8-AgPF <sub>6</sub> .....	29
<b>Table S8</b> Selected bond lengths (Å) and bond angles (°) for (R)-6-Zn(NO <sub>3</sub> ) <sub>2</sub> .....	29
<b>References</b> .....	30

## Experimental Procedures

### General.

All chemicals and solvents used in the syntheses were of reagent grade and were used without further purification. NMR spectra were recorded on a JEOL ECP400 spectrometer (400 MHz). The FAB mass spectrum was obtained on a JEOL 600H mass spectrometer. The CD spectra were measured on a JASCO J-820 CD spectrophotometer. CD spectra were determined over the range of 240-350 nm using a quartz cell with 1.0 mm path length. Scans were taken at a rate of 50 nm/min with a sampling interval of 0.1 nm and the response time of 2 s. The absorption spectra were recorded on a JASCO V-550 UV-visible spectrophotometer. UV-vis titration experiments. The path length of the cuvette was 1 cm. Stability constants were calculated using HyperSpec™ ver. 1.1.33.<sup>1</sup> Optical rotations were measured on a digital polarimeter JASCO DIP-360. A sodium lamp ( $\lambda = 589$  nm) was used as a light source. The elemental analysis was carried out on a Yanako MT-6 CHN Micro Corder.



**Scheme S1** Syntheses of chiral tetra-armed cyclens.

### Synthesis of (R)-6.

30 mL of a diisobutylaluminum hydride solution in THF (1 M) was slowly added to a 3-methyl-(3R)-1,4,7,10-tetraazacyclododecane-2,6-dione ((R)-4)<sup>2,3</sup> (0.645 g, 3.01 mmol) at 0 °C and then stirred for 1 day at room temperature under argon atmosphere. The reaction mixture was cooled to 0 °C, and then benzene (90 mL) was added, and then sodium fluoride (5.04 g, 120 mmol) and 1.5 mL of water (83.3 mmol) were added to the reaction mixture. The reaction mixture was stirred for 4 h at room temperature, and then evaporated to obtain (R)-5 in the crude state. FAB-MS ( $m/z$ ) (matrix: DTT:TG = 1:1): 187 ( $[M+1]^+$ , 100%). The crude (R)-5, *p*-tolualdehyde (2.17 g, 18.1 mmol), sodium triacetoxyborohydride (5.09 g, 24.0 mmol) were added to 1,2-dichloroethane (30 mL) and stirred for 5

days at room temperature under argon atmosphere. The saturated sodium hydrogen carbonate solution was added until pH 11 and extracted with chloroform. The organic layer was separated and dried over anhydrous sodium sulfate, filtered, and then evaporated. After silica gel column chromatography (chloroform:methanol:aqueous ammonia = 5:1:0.06) was performed to give the (*R*)-**6**. Yield: 27%. Mp: 86.0-88.0 °C.  $[\alpha]^{20}_D = +32.6$  ( $c = 0.301$ ,  $\text{CHCl}_3$ :  $\text{MeOH} = 1:19$ ).  $^1\text{H NMR}$  (400 MHz,  $\text{CDCl}_3$ ):  $\delta$  7.31-7.00 (m, 16H), 3.60-3.16 (m, 9H), 2.96-2.20 (m, 25H), 2.04 (dd,  $J_1 = 13.0$  Hz,  $J_2 = 4.0$  Hz, 1H), 0.88 (d,  $J = 6.6$  Hz, 3H).  $^{13}\text{C NMR}$  (100 MHz,  $\text{CDCl}_3$ ):  $\delta$  138.0, 136.9, 135.9, 129.0, 128.9, 128.7, 128.6, 60.1, 59.7, 59.6, 59.0, 54.2, 53.8, 52.4, 52.3, 47.3, 21.1, 11.6. FAB-MS ( $m/z$ ) (matrix: DTT:TG = 1:2): 603 ( $[\text{M}+1]^+$ , 100%). Anal. Calcd. For  $[\text{C}_{41}\text{H}_{54}\text{N}_4]$ : C, 81.68; H, 9.03; N, 9.26. Found: C, 81.38; H, 9.06; N, 9.24%.

### Synthesis of (*S*)-**6**.

30 mL of a diisobutylaluminum hydride solution in THF (1 M) was slowly added to a 3-methyl-(3*S*)-1,4,7,10-tetraazacyclododecane-2,6-dione ((*S*)-**4**)<sup>[2,3]</sup> (0.642 g, 3.00 mmol) at 0 °C and then stirred for 1 day at room temperature under argon atmosphere. The reaction mixture was cooled to 0 °C, and then benzene (90 mL) was added, and then sodium fluoride (5.04 g, 120 mmol) and 1.5 mL of water (83.3 mmol) were added to the reaction mixture. The reaction mixture was stirred for 4 h at room temperature, and then evaporated to obtain (*S*)-**5** in the crude state. FAB-MS ( $m/z$ ) (matrix: DTT:TG = 1:1): 187 ( $[\text{M}+1]^+$ , 100%). The crude (*S*)-**5**, *p*-tolualdehyde (2.17 g, 18.1 mmol), sodium triacetoxyborohydride (5.09 g, 24.0 mmol) were added to 1,2-dichloroethane (30 mL) and stirred for 5 days at room temperature under argon atmosphere. The saturated sodium hydrogen carbonate solution was added until pH 11 and extracted with chloroform. The organic layer was separated and dried over anhydrous sodium sulfate, filtered, and then evaporated. After silica gel column chromatography (chloroform:methanol:aqueous ammonia = 5:1:0.06) was performed to give the (*R*)-**6**. Yield: 28%. Mp: 84.5-86.5 °C.  $[\alpha]^{20}_D = -32.3$  ( $c = 0.301$ ,  $\text{CHCl}_3$ :  $\text{MeOH} = 1:19$ ).  $^1\text{H NMR}$  (400 MHz,  $\text{CDCl}_3$ ):  $\delta$  7.31-7.00 (m, 16H), 3.60-3.16 (m, 9H), 2.96-2.20 (m, 25H), 2.04 (dd,  $J_1 = 13.0$  Hz,  $J_2 = 4.0$  Hz, 1H), 0.88 (d,  $J = 6.6$  Hz, 3H).  $^{13}\text{C NMR}$  (100 MHz,  $\text{CDCl}_3$ ):  $\delta$  138.0, 136.9, 135.9, 129.0, 128.9, 128.7, 128.6, 60.1, 59.7, 59.6, 59.0, 54.2, 53.8, 52.5, 52.3, 47.3, 21.1, 11.6. FAB-MS ( $m/z$ ) (matrix: DTT:TG = 1:2): 603 ( $[\text{M}+1]^+$ , 100%). Anal. Calcd. For  $[\text{C}_{41}\text{H}_{54}\text{N}_4]$ : C, 81.68; H, 9.03; N, 9.26. Found: C, 81.28; H, 9.07; N, 9.28%.

### Synthesis of (*R*)-**7**.

The procedure was the same as for (*R*)-**6**, but with the use of benzaldehyde instead of *p*-tolualdehyde. Yield: 25%. Mp: 98.0-99.2 °C.  $[\alpha]^{20}_D = +23.2$  ( $c = 0.301$ ,  $\text{CHCl}_3$ :  $\text{MeOH} = 1:19$ ).  $^1\text{H NMR}$  (400 MHz,  $\text{CDCl}_3$ ):  $\delta$  7.45-7.10 (m, 20H), 3.65-3.20 (m, 9H), 3.00-2.30 (m, 13H), 2.06 (dd,  $J_1 = 13.1$  Hz,  $J_2 = 4.1$  Hz, 1H), 0.90 (d,  $J = 6.6$  Hz, 3H).  $^{13}\text{C NMR}$  (100 MHz,  $\text{CDCl}_3$ ):  $\delta$  141.0, 140.0, 129.0, 128.9, 128.0, 127.9, 126.5, 126.4, 60.4, 60.0, 59.2, 54.5, 54.0, 52.8, 52.5, 47.4, 11.4. FAB-MS ( $m/z$ ) (matrix: DTT:TG = 1:2): 547 ( $[\text{M}+1]^+$ , 100%). Anal. Calcd. For  $[\text{C}_{37}\text{H}_{46}\text{N}_4]$ : C, 81.27; H, 8.48; N, 10.25. Found: C, 81.37; H, 8.54; N, 10.26%.

### Synthesis of (*S*)-**7**.

The procedure was the same as for (*S*)-**6**, but with the use of benzaldehyde instead of *p*-tolualdehyde. Yield: 20%. Mp: 91.7-92.5 °C.  $[\alpha]^{20}_D = -26.8$  ( $c = 0.547$ ,  $\text{CHCl}_3$ :  $\text{MeOH} = 1:19$ ).  $^1\text{H NMR}$  (400 MHz,  $\text{CDCl}_3$ ):  $\delta$  7.45-7.10 (m, 20H), 3.65-3.20 (m, 9H), 3.00-2.30 (m, 13H), 2.06 (dd,  $J_1 = 13.1$  Hz,  $J_2 = 4.1$  Hz, 1H), 0.90 (d,  $J = 6.6$  Hz, 3H).  $^{13}\text{C NMR}$  (100 MHz,  $\text{CDCl}_3$ ):  $\delta$  141.0, 140.0, 129.0, 128.9, 128.0, 127.9, 126.5, 126.4, 60.5,

60.0, 59.2, 54.5, 54.0, 52.8, 52.5, 47.4, 11.5. FAB-MS ( $m/z$ ) (matrix: DTT:TG = 1:2): 547 ( $[M+1]^+$ , 100%). Anal. Calcd. For  $[C_{37}H_{46}N_4+0.1H_2O]$ : C, 81.01; H, 8.49; N, 10.21. Found: C, 80.77; H, 8.39; N, 10.19%.

#### Synthesis of (*R*)-8.

The procedure was the same as for (*R*)-6, but with the use of 4-fluorobenzaldehyde instead of *p*-tolualdehyde. The purification of the product was performed by silica gel column chromatography (chloroform:methanol = 10:1). Yield: 22%. Mp: 115.0-117.0 °C.  $[\alpha]_D^{20} = +19.7$  ( $c = 0.309$ ,  $CHCl_3$ : MeOH = 1:19).  $^1H$  NMR (400 MHz,  $CDCl_3$ ):  $\delta$  7.40-7.16 (m, 8H), 7.03-6.82 (m, 8H), 3.60-3.10 (m, 9H), 2.92-2.30 (m, 13H), 2.03 (dd,  $J_1 = 13.1$  Hz,  $J_2 = 4.0$  Hz, 1H), 0.89 (d,  $J = 6.6$  Hz, 3H).  $^{13}C$  NMR (100 MHz,  $CDCl_3$ ):  $\delta$  163.0, 160.5, 136.4, 135.5, 135.4, 130.3, 130.2, 114.8, 114.6, 59.7, 59.2, 53.7, 52.9, 52.7, 52.5, 52.4, 47.3, 11.4. FAB-MS ( $m/z$ ) (matrix: DTT:TG = 1:2): 619 ( $[M+1]^+$ , 100%). Anal. Calcd. For  $[C_{37}H_{42}N_4F_4]$ : C, 71.82; H, 6.84; N, 9.05. Found: C, 71.82; H, 6.98; N, 8.90%.

#### Synthesis of (*S*)-8.

The procedure was the same as for (*S*)-6, but with the use of 4-fluorobenzaldehyde instead of *p*-tolualdehyde. The purification of the product was performed by silica gel column chromatography (chloroform:methanol = 10:1). Yield: 21%. Mp: 116.0-117.5 °C.  $[\alpha]_D^{20} = -18.4$  ( $c = 0.309$ ,  $CHCl_3$ : MeOH = 1:19).  $^1H$  NMR (400 MHz,  $CDCl_3$ ):  $\delta$  7.40-7.16 (m, 8H), 7.03-6.82 (m, 8H), 3.60-3.10 (m, 9H), 2.92-2.30 (m, 13H), 2.03 (dd,  $J_1 = 13.1$  Hz,  $J_2 = 4.0$  Hz, 1H), 0.89 (d,  $J = 6.6$  Hz, 3H).  $^{13}C$  NMR (100 MHz,  $CDCl_3$ ):  $\delta$  163.0, 160.5, 136.4, 135.5, 135.4, 130.3, 130.2, 114.8, 114.6, 59.7, 59.2, 53.7, 52.9, 52.7, 52.5, 52.4, 47.3, 11.4. FAB-MS ( $m/z$ ) (matrix: DTT:TG = 1:2): 619 ( $[M+1]^+$ , 100%). Anal. Calcd. For  $[C_{37}H_{42}N_4F_4]$ : C, 71.82; H, 6.84; N, 9.05. Found: C, 71.99; H, 6.96; N, 8.96%.

#### Synthesis of (*R*)-9.

The procedure was the same as for (*R*)-6, but with the use of 3,5-difluorobenzaldehyde instead of *p*-tolualdehyde. The purification of the product was performed by silica gel column chromatography (chloroform:methanol = 10:1). Yield: 12%. Mp: 87.2-90.0 °C.  $[\alpha]_D^{20} = +20.6$  ( $c = 0.691$ ,  $CHCl_3$ : MeOH = 1:19).  $^1H$  NMR (400 MHz,  $CDCl_3$ ):  $\delta$  6.95 (dd,  $J_1 = 8.0$  Hz,  $J_2 = 2.0$  Hz, 2H), 6.88 (dd,  $J_1 = 8.0$  Hz,  $J_2 = 2.0$  Hz, 2H), 6.86 (dd,  $J_1 = 8.0$  Hz,  $J_2 = 2.0$  Hz, 2H), 6.82 (dd,  $J_1 = 8.0$  Hz,  $J_2 = 2.0$  Hz, 2H), 6.71-6.60 (m, 4H) 3.60-3.20 (m, 9H), 2.91-2.37 (m, 13H), 2.10 (dd,  $J_1 = 13.2$  Hz,  $J_2 = 4.1$  Hz, 1H), 0.94 (d,  $J = 6.6$  Hz, 3H).  $^{13}C$  NMR (100 MHz,  $CDCl_3$ ):  $\delta$  164.3, 164.1, 161.8, 161.7, 161.6, 145.2, 145.1, 145.0, 144.1, 144.0, 143.9, 143.8, 111.5, 111.4, 111.3, 111.2, 111.1, 111.0, 102.5, 102.4, 102.2, 102.1, 102.0, 101.9, 60.1, 59.5, 59.4, 54.1, 53.9, 53.1, 53.0, 52.8, 47.8, 11.6. FAB-MS ( $m/z$ ) (matrix: DTT:TG = 1:2): 691 ( $[M+1]^+$ , 100%). Anal. Calcd. For  $[C_{37}H_{38}N_4F_8]$ : C, 64.34; H, 5.55; N, 8.11. Found: C, 64.69; H, 5.76; N, 7.77%.

#### Synthesis of (*S*)-9.

The procedure was the same as for (*S*)-6, but with the use of 3,5-difluorobenzaldehyde instead of *p*-tolualdehyde. The purification of the product was performed by silica gel column chromatography (chloroform:methanol = 10:1). Yield: 7%. Mp: 86.0-87.2 °C.  $[\alpha]_D^{20} = -25.9$  ( $c = 0.691$ ,  $CHCl_3$ : MeOH = 1:19).  $^1H$  NMR (400 MHz,  $CDCl_3$ ):  $\delta$  6.95 (dd,  $J_1 = 8.0$  Hz,  $J_2 = 2.0$  Hz, 2H), 6.88 (dd,  $J_1 = 8.0$  Hz,  $J_2 = 2.0$  Hz, 2H), 6.86 (dd,  $J_1 = 8.0$  Hz,  $J_2 = 2.0$  Hz, 2H), 6.82 (dd,  $J_1 = 8.0$  Hz,  $J_2 = 2.0$  Hz, 2H), 6.71-6.60 (m, 4H) 3.60-3.20 (m, 9H), 2.91-2.37 (m, 13H), 2.10 (dd,  $J_1 = 13.2$  Hz,  $J_2 = 4.1$  Hz, 1H), 0.94 (d,  $J = 6.6$  Hz, 3H).  $^{13}C$  NMR (100 MHz,  $CDCl_3$ ):  $\delta$  164.3, 164.2, 164.1, 161.8, 161.7,

161.6, 145.2, 145.1, 145.0, 144.0, 143.9, 143.8, 111.5, 111.4, 111.3, 111.2, 111.1, 111.0, 102.5, 102.4, 102.2, 102.1, 102.0, 101.9, 60.1, 59.5, 59.4, 54.1, 53.9, 53.1, 53.0, 52.8, 47.8, 11.6. FAB-MS ( $m/z$ ) (matrix: DTT:TG = 1:2): 691 ( $[M+1]^+$ , 100%). Anal. Calcd. For  $[C_{37}H_{38}N_4F_8+0.1H_2O]$ : C, 64.17; H, 5.56; N, 8.09. Found: C, 63.92; H, 5.65; N, 8.05%.

#### **Preparation of (R)-6-AgPF<sub>6</sub>.**

AgPF<sub>6</sub> (6.32 mg, 0.025 mmol) in methanol (1 mL) was added to a solution of **(R)-6** (15.1 mg, 0.025 mmol) in chloroform (1 mL). The white precipitate obtained was dissolved in acetonitrile (2 mL). Slow evaporation of the solution afforded a colorless crystalline product suitable for X-ray analysis. Mp: 222-224 °C. Anal. calcd. for  $[C_{41}H_{54}AgN_4PF_6]$ : C, 57.55; H, 6.36; N, 6.55. Found: C, 57.73; H, 6.49; N, 6.40%.

#### **Preparation of (S)-6-AgPF<sub>6</sub>.**

AgPF<sub>6</sub> (6.32 mg, 0.025 mmol) in methanol (1 mL) was added to a solution of **(S)-6** (15.1 mg, 0.025 mmol) in chloroform (1 mL). Slow evaporation of the solution afforded a colorless crystalline product suitable for X-ray analysis. Mp: 231-233 °C. Anal. calcd. for  $[C_{41}H_{54}AgN_4P_1F_6+0.3H_2O]$ : C, 57.19; H, 6.39; N, 6.51. Found: C, 56.92; H, 6.27; N, 6.60%.

#### **Preparation of (S)-7-AgBF<sub>4</sub>.**

AgBF<sub>4</sub> (4.87 mg, 0.025 mmol) in ethanol (1 mL) was added to a solution of **(S)-7** (13.7 mg, 0.025 mmol) in 1,2-dichloroethane (1 mL). Slow evaporation of the solution afforded a colorless crystalline product suitable for X-ray analysis. Mp: 205-207 °C. Anal. calcd. for  $[C_{37}H_{46}AgN_4B_1F_4]$ : C, 59.94; H, 6.25; N, 7.56. Found: C, 60.21; H, 6.18; N, 7.36%.

#### **Preparation of (R)-8-AgPF<sub>6</sub>.**

AgPF<sub>6</sub> (6.35 mg, 0.025 mmol) in methanol (1 mL) was added to a solution of **(R)-8** (15.5 mg, 0.025 mmol) in dichloromethane (1 mL). Slow evaporation of the solution afforded a colorless crystalline product suitable for X-ray analysis. Mp: 229-231 °C. Anal. calcd. for  $[C_{37}H_{42}AgN_4P_1F_{10}]$ : C, 50.99; H, 4.86; N, 6.43. Found: C, 51.27; H, 4.90; N, 6.25%.

#### **Preparation of (R)-6-Zn(NO<sub>3</sub>)<sub>2</sub>.**

Zn(NO<sub>3</sub>)<sub>2</sub>·6H<sub>2</sub>O (7.45 mg, 0.025 mmol) in methanol (1 mL) was added to a solution of **(R)-6** (15.1 mg, 0.025 mmol) in chloroform (1 mL). Slow evaporation of the solution afforded a colorless crystalline product suitable for X-ray analysis. Mp: 222-224 °C. Anal. calcd. for  $[C_{41}H_{54}ZnN_6O_6\cdot H_2O]$ : C, 60.77; H, 6.97; N, 10.37. Found: C, 60.66; H, 6.47; N, 10.16%.

## Results and Discussion

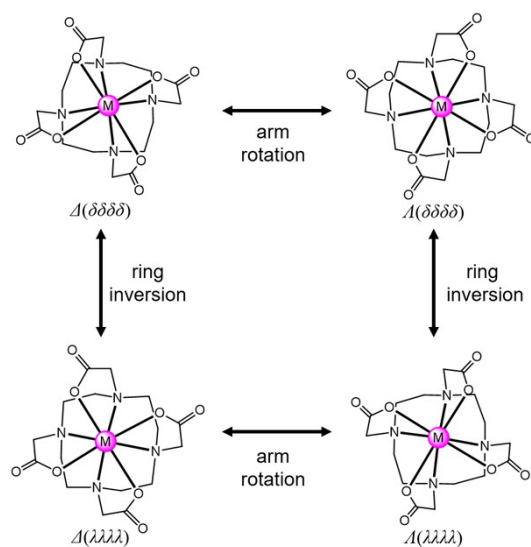


**Fig. S1** Four isomers of metal complexes with a tetra-armed cyclen.

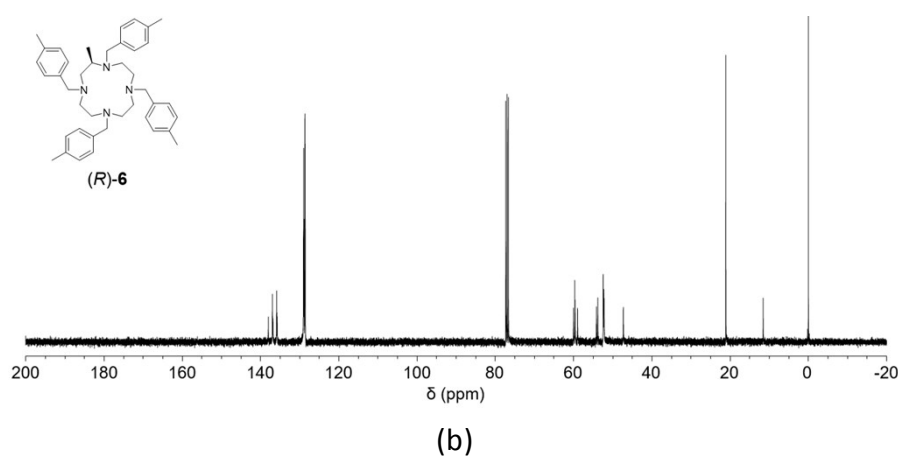
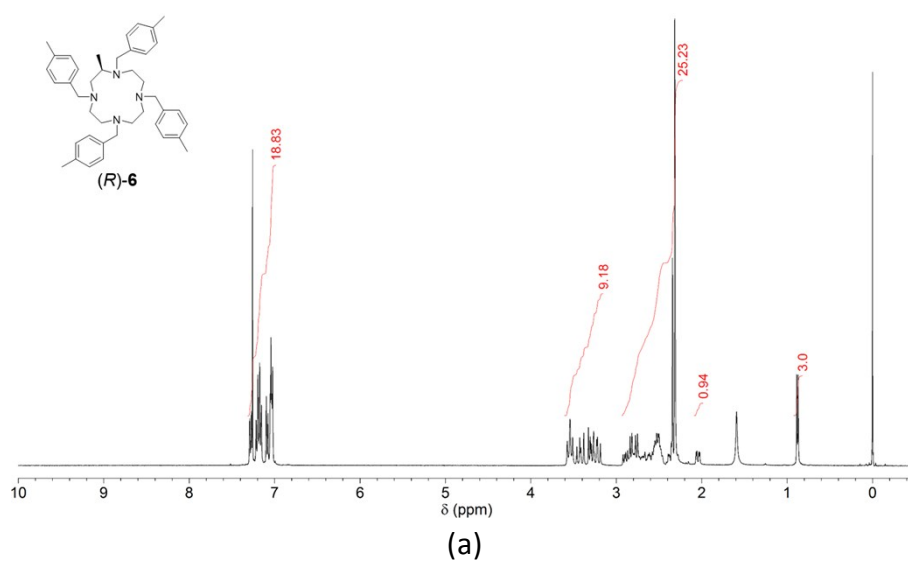


**Fig. S2** (a)  $^1\text{H}$  and (b)  $^{13}\text{C}$  NMR spectra of  $(R)$ -6 in  $\text{CDCl}_3$ .

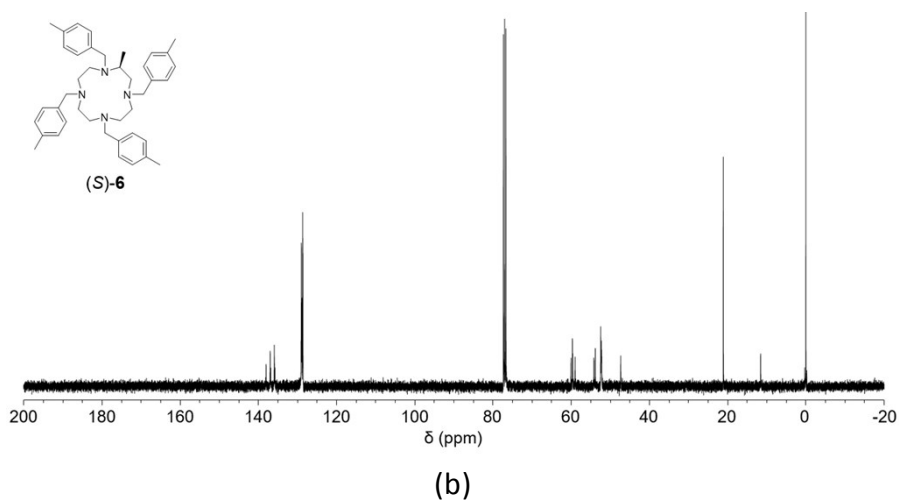
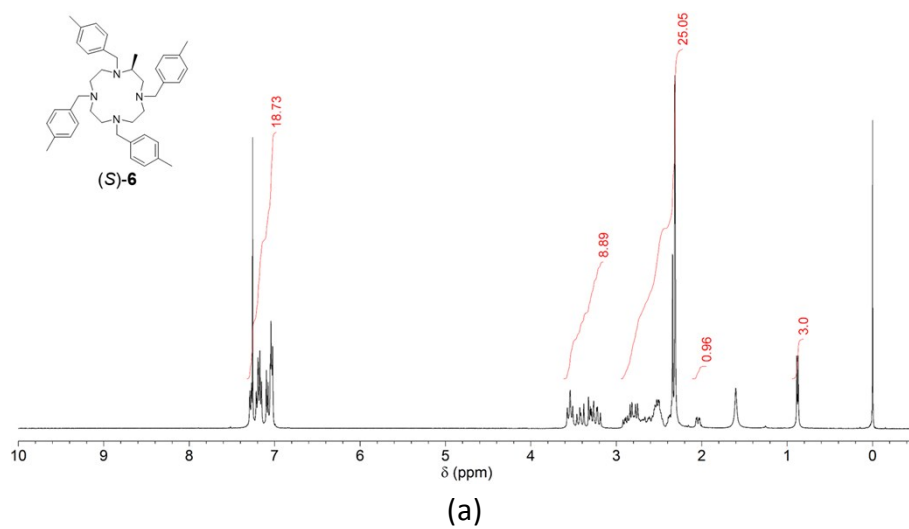


**Fig. S3** (a)  $^1\text{H}$  and (b)  $^{13}\text{C}$  NMR spectra of (*S*)-**6** in  $\text{CDCl}_3$ .



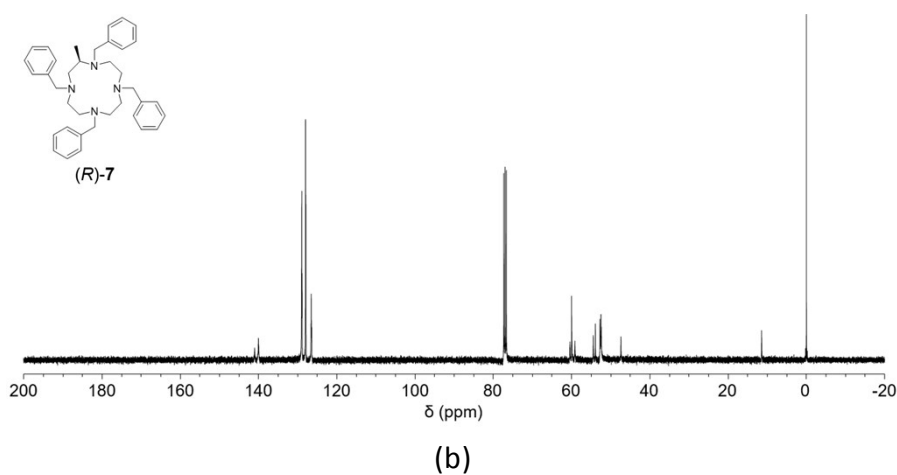
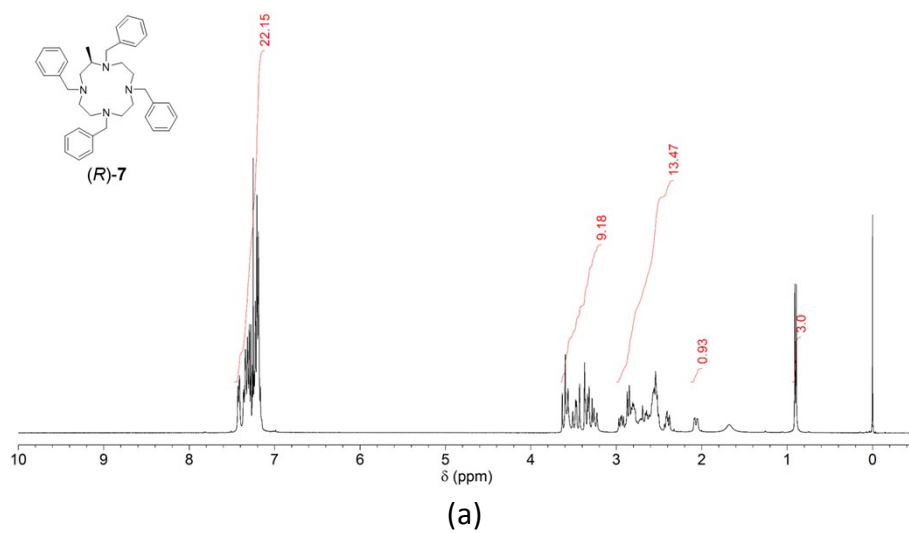


**Fig. S4** (a)  $^1\text{H}$  and (b)  $^{13}\text{C}$  NMR spectra of (*R*)-**7** in  $\text{CDCl}_3$ .

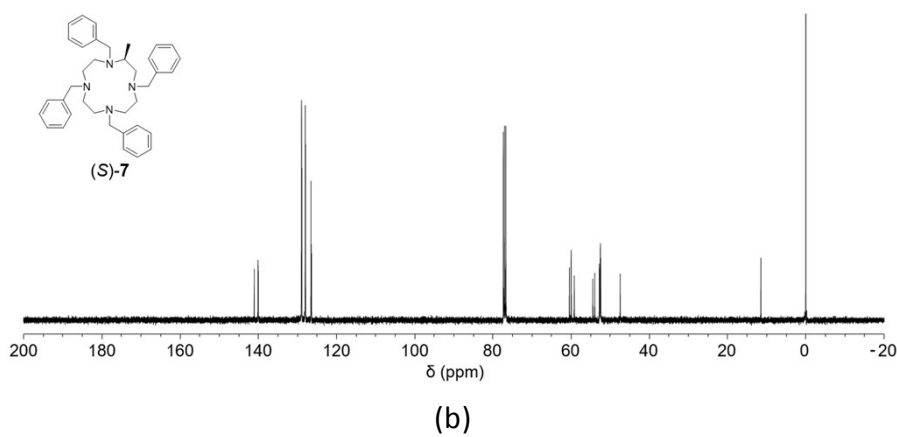
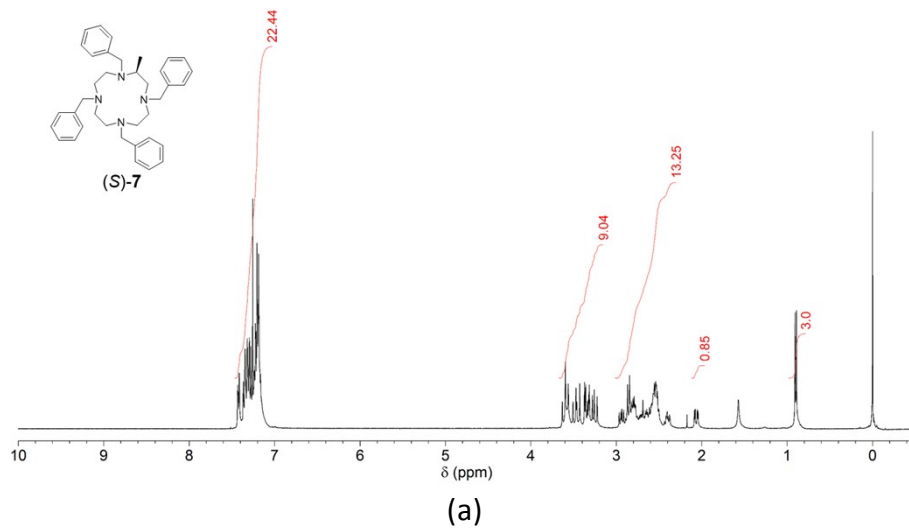


**Fig. S5** (a)  $^1\text{H}$  and (b)  $^{13}\text{C}$  NMR spectra of (*S*)-**7** in  $\text{CDCl}_3$ .

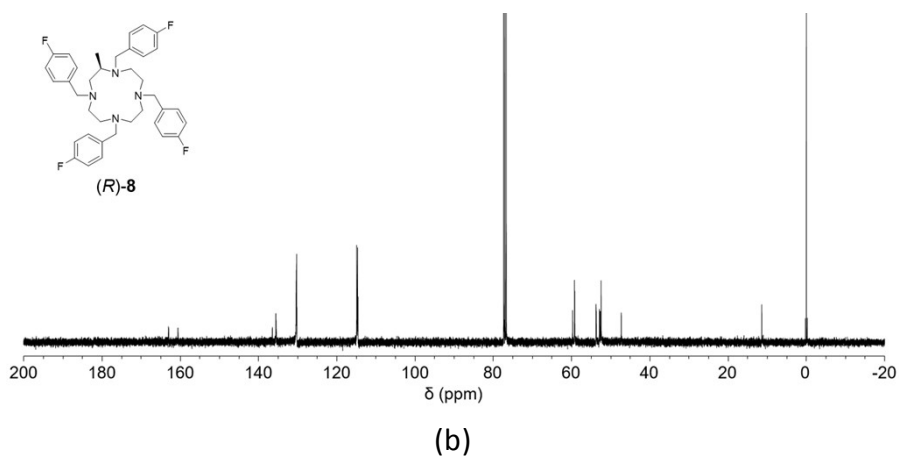
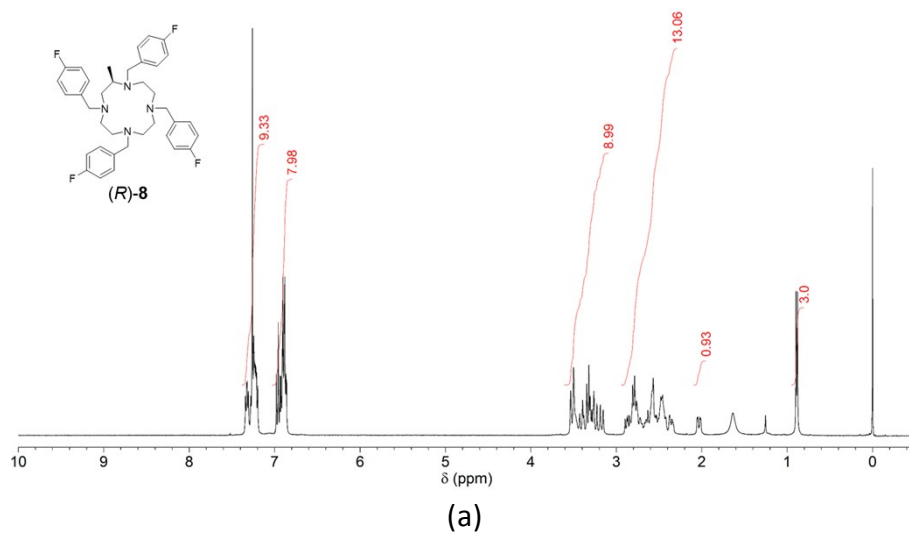


**Fig. S6** (a)  $^1\text{H}$  and (b)  $^{13}\text{C}$  NMR spectra of (*R*)-**8** in  $\text{CDCl}_3$ .

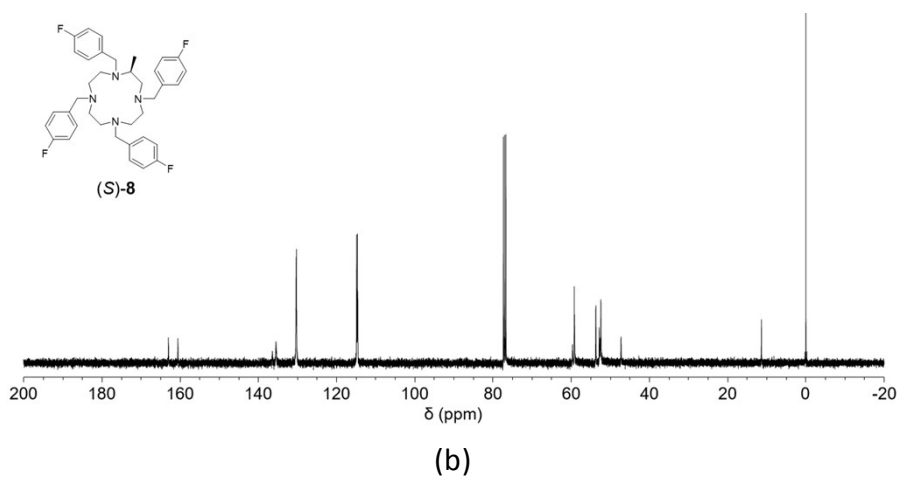
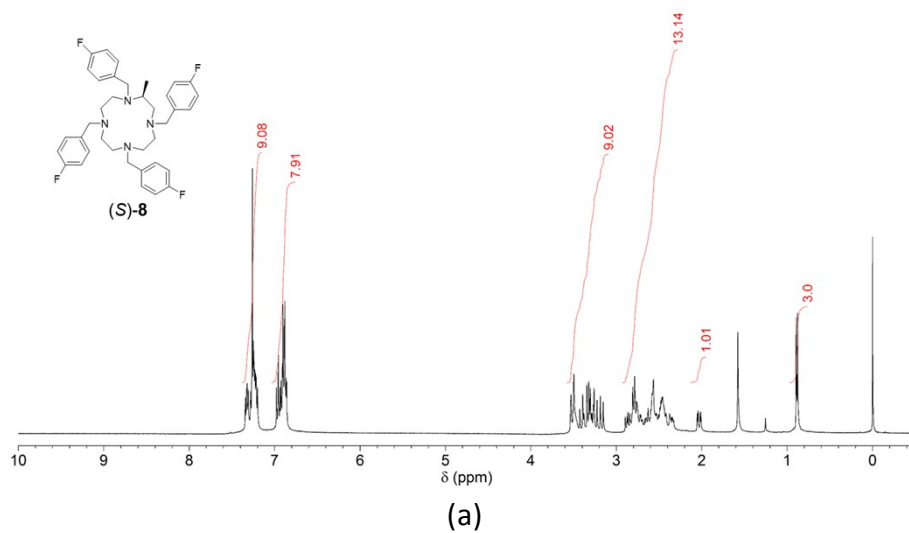


**Fig. S7** (a)  $^1\text{H}$  and (b)  $^{13}\text{C}$  NMR spectra of (*S*)-**8** in  $\text{CDCl}_3$ .

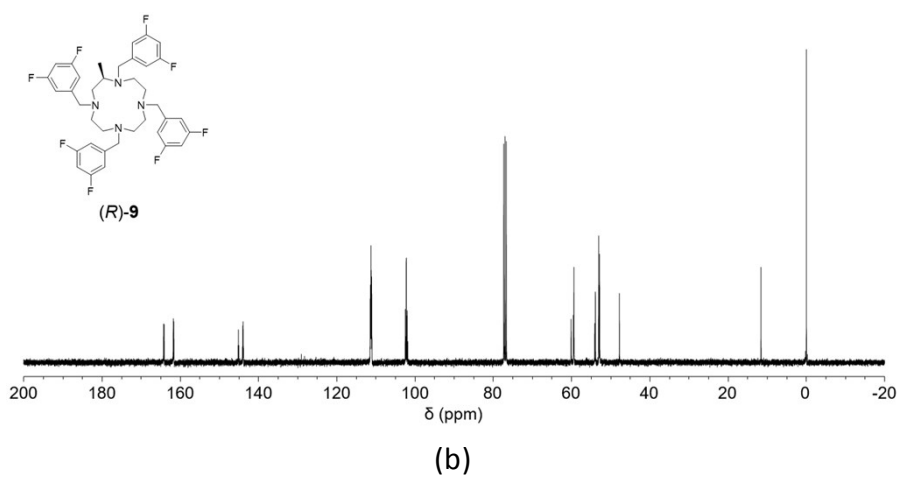
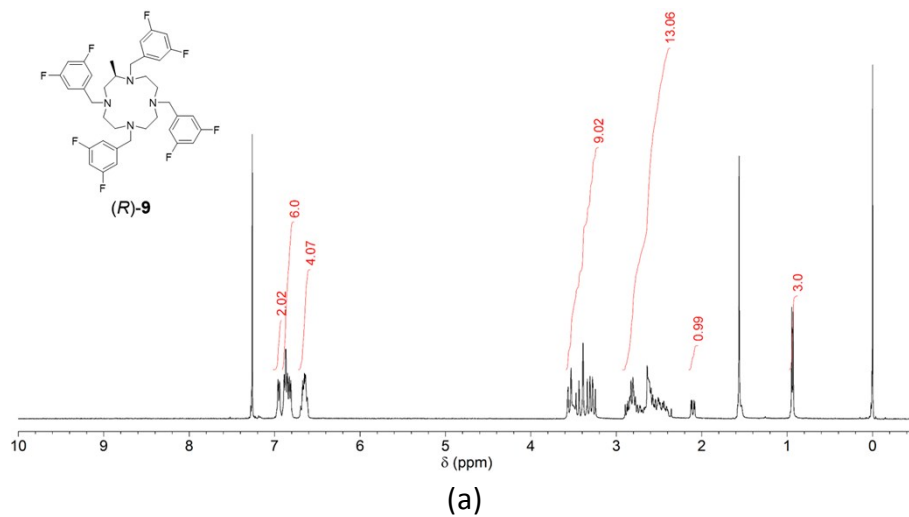


**Fig. S8** (a)  $^1\text{H}$  and (b)  $^{13}\text{C}$  NMR spectra of (*R*)-**9** in  $\text{CDCl}_3$ .

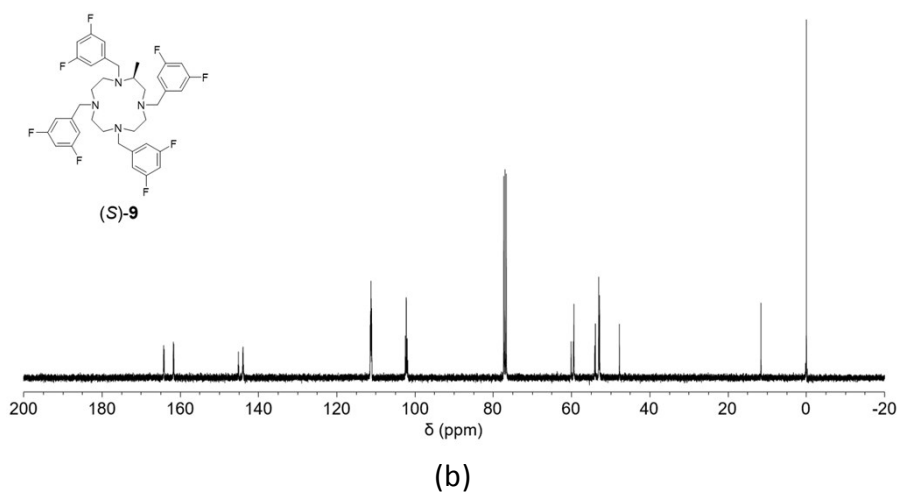
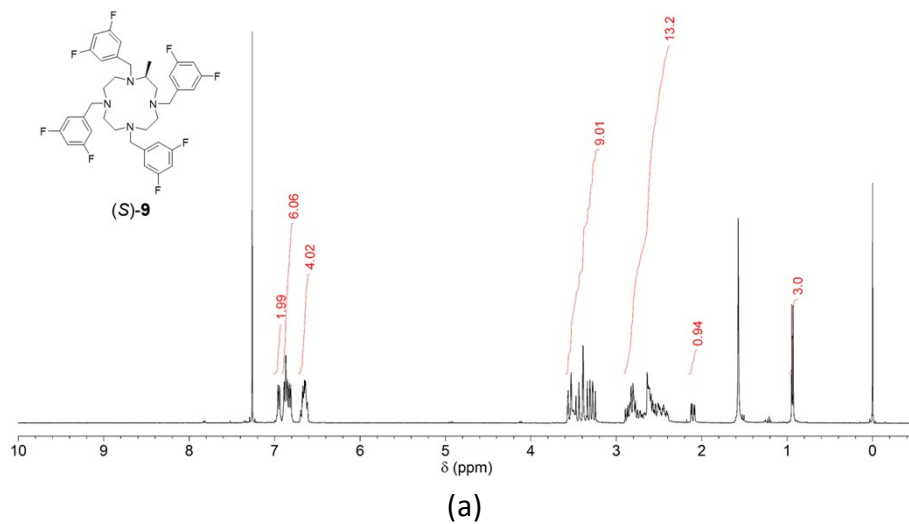


**Fig. S9** (a)  $^1\text{H}$  and (b)  $^{13}\text{C}$  NMR spectra of (S)-9 in  $\text{CDCl}_3$ .

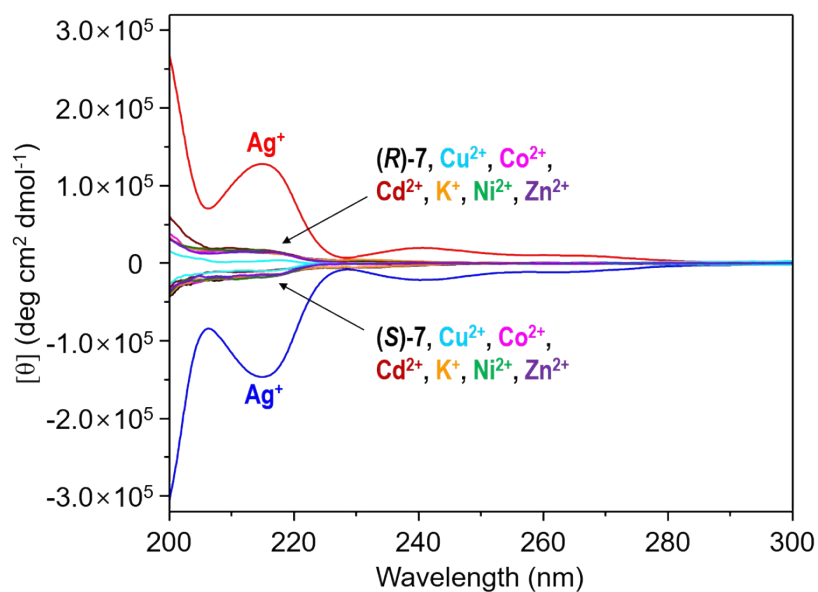


**Fig. S10** CD spectra of (*R*)-**7** and (*S*)-**7** (2.5 mM) in the presence of metal triflates (1.0 equivalents) in  $\text{CHCl}_3:\text{CH}_3\text{OH}$  (1:19).

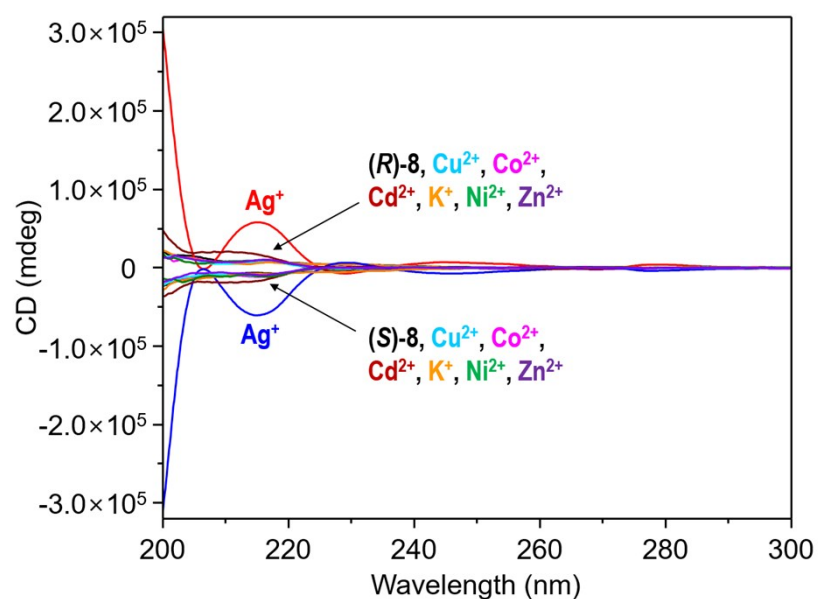


**Fig. S11** CD spectra of (*R*)-**8** and (*S*)-**8** (2.5 mM) in the presence of metal triflates (1.0 equivalents) in  $\text{CHCl}_3:\text{CH}_3\text{OH}$  (1:19).

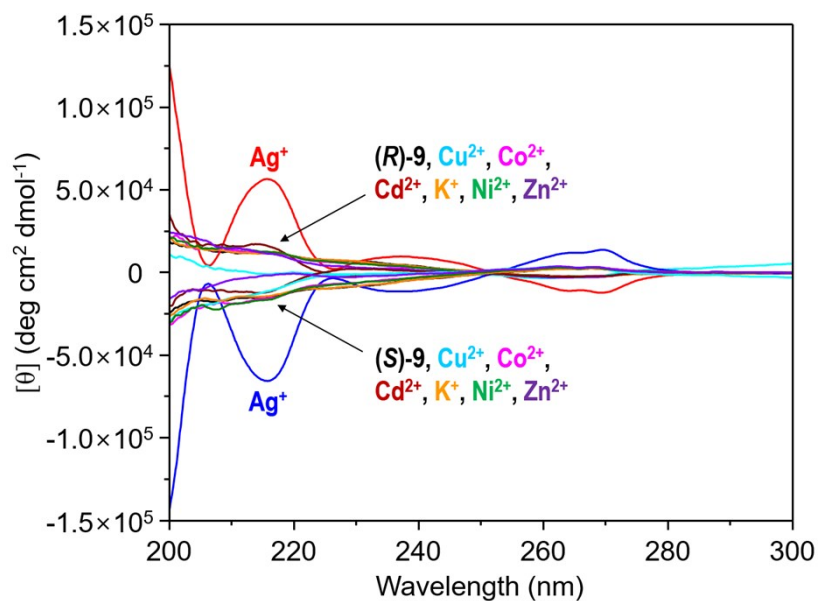


**Fig. S12** CD spectra of (R)-9 and (S)-9 (2.5 mM) in the presence of metal triflates (1.0 equivalents) in CHCl<sub>3</sub>:CH<sub>3</sub>OH (1:19).

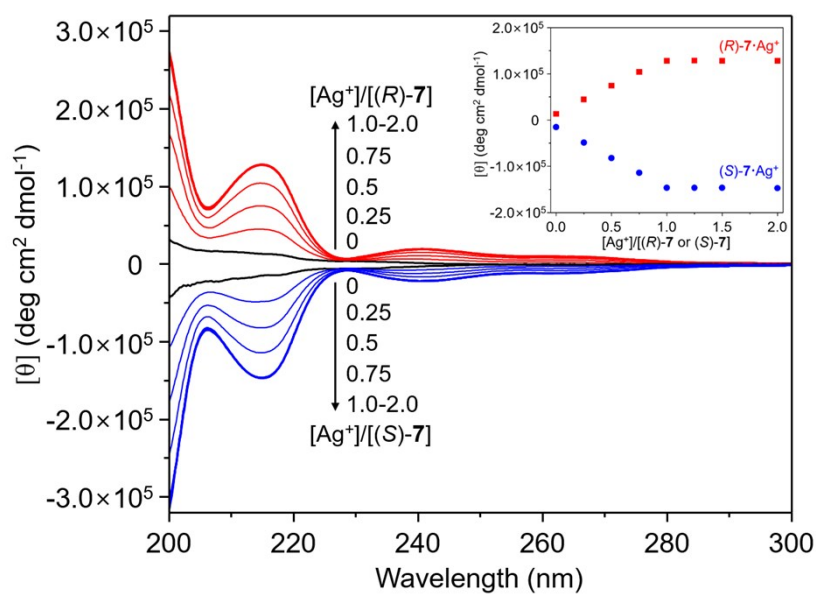


**Fig. S13** CD spectral changes of (R)-7 and (S)-7 (2.5 mM) upon addition of silver(I) in CHCl<sub>3</sub>:CH<sub>3</sub>OH (1:19). (inset) titration curves at 215 nm.



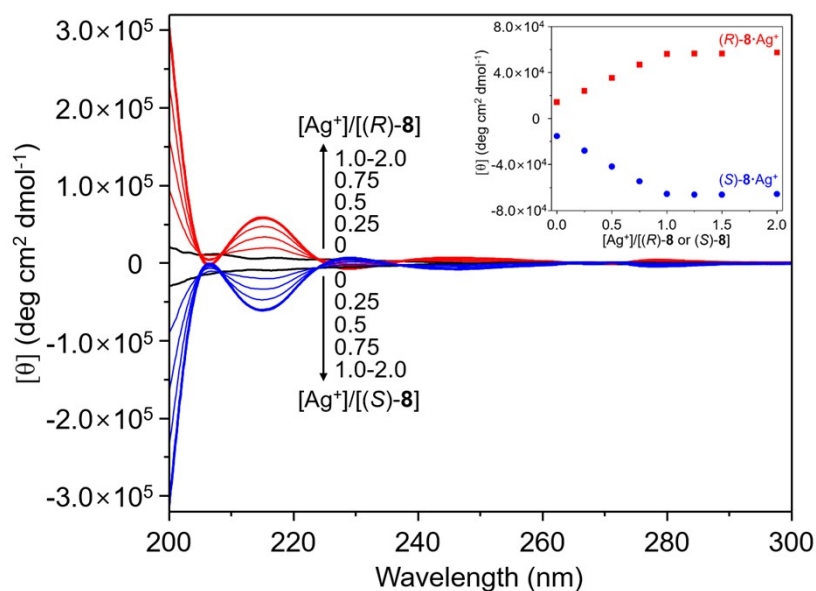


**Fig. S14** CD spectral changes of (R)-8 and (S)-8 (2.5 mM) upon addition of silver(I) in CHCl<sub>3</sub>:CH<sub>3</sub>OH (1:19). (inset) titration curves at 215 nm.

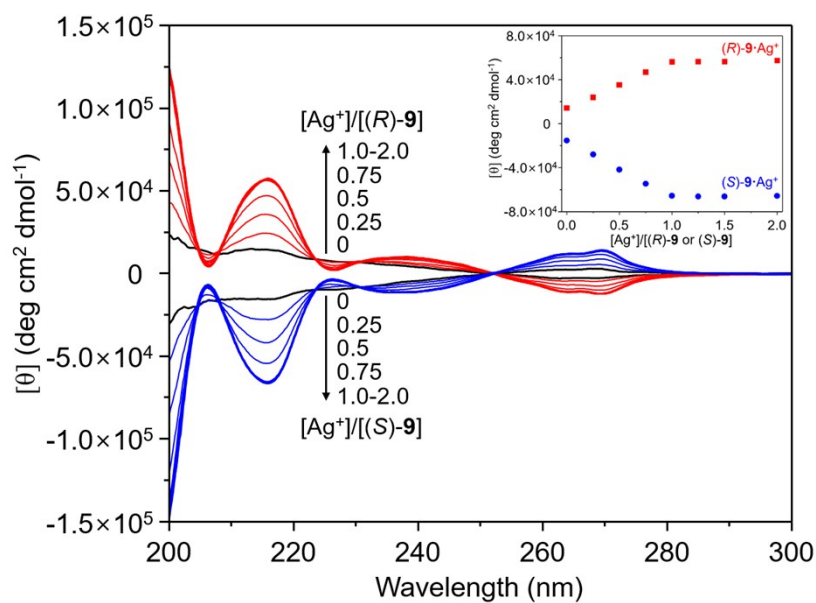


**Fig. S15** CD spectral changes of (R)-9 and (S)-9 (2.5 mM) upon addition of silver(I) in CHCl<sub>3</sub>:CH<sub>3</sub>OH (1:19). (inset) titration curves at 216 nm.

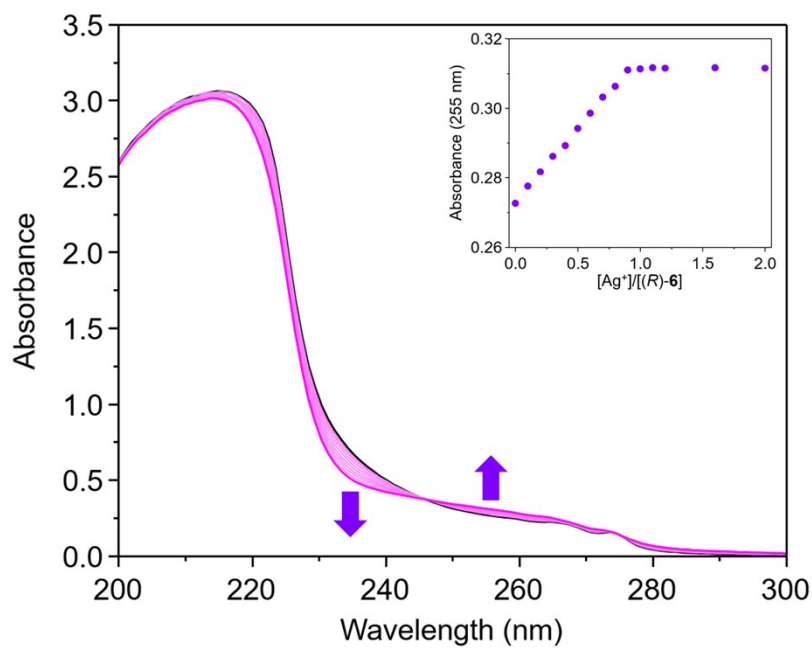


**Fig. S16** UV-Vis spectral changes of (R)-6 (0.1 mM) upon addition of silver(I) triflate in CH<sub>3</sub>CN. (inset) titration curves at 255 nm.

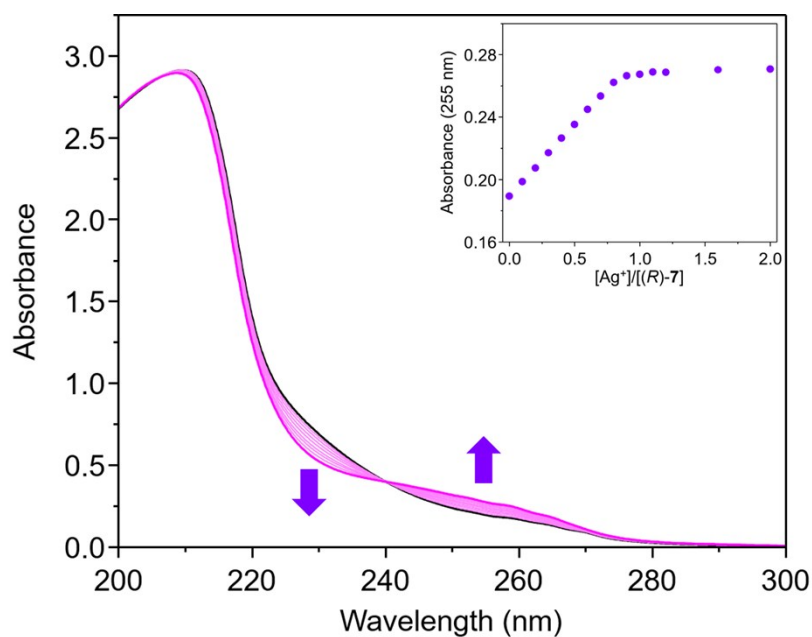


**Fig. S17** UV-Vis spectral changes of (R)-7 (0.1 mM) upon addition of silver(I) triflate in CH<sub>3</sub>CN. (inset) titration curves at 255 nm.

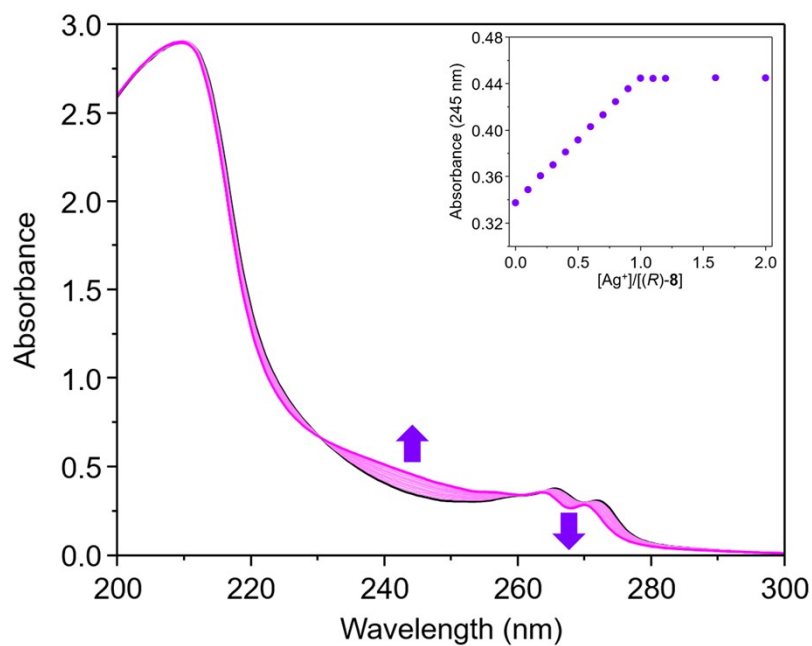


**Fig. S18** UV-Vis spectral changes of (R)-8 (0.1 mM) upon addition of silver(I) triflate in CH<sub>3</sub>CN. (inset) titration curves at 245 nm.

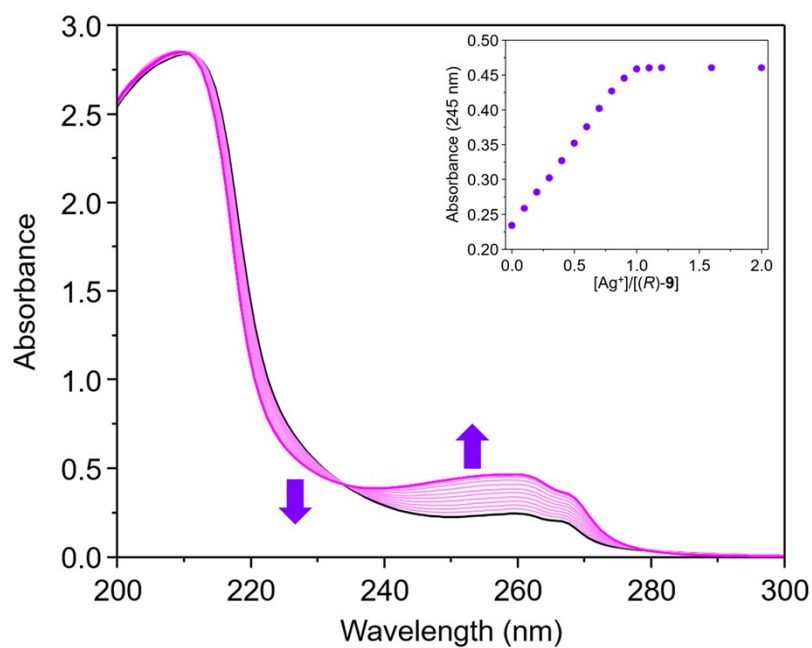


**Fig. S19** UV-Vis spectral changes of (R)-9 (0.1 mM) upon addition of silver(I) triflate in CH<sub>3</sub>CN. (inset) titration curves at 245 nm.

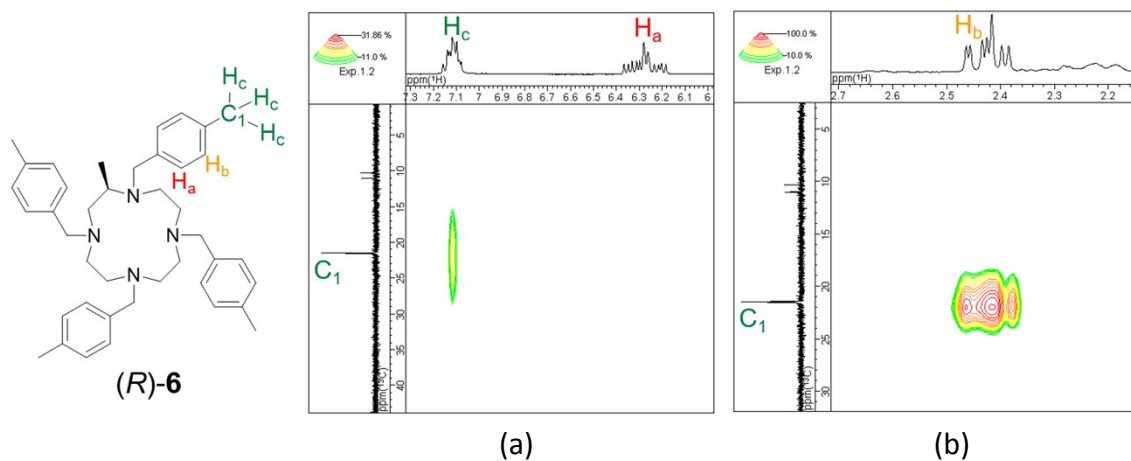


**Fig. S20** (a) HMBC and (b) HMQC spectra of (R)-6 (5  $\mu$ M) with silver(I) triflate (1.0 equiv.).

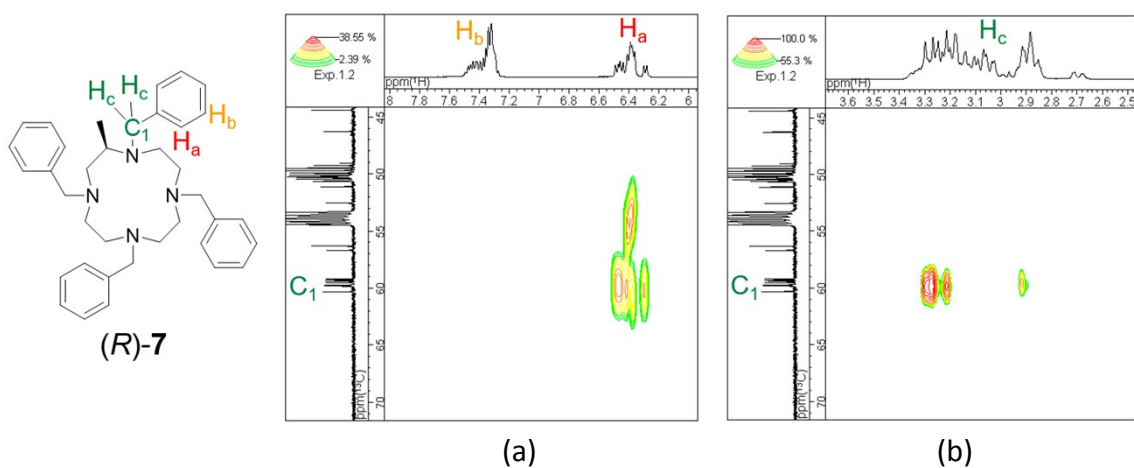


**Fig. S21** (a) HMBC and (b) HMQC spectra of (R)-7 (5  $\mu$ M) with silver(I) triflate (1.0 equiv.).

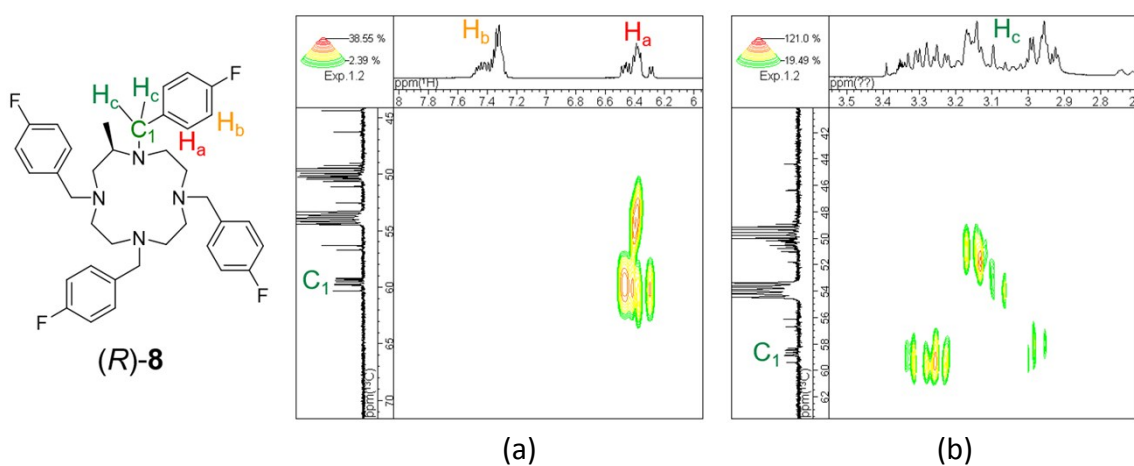


**Fig. S22** (a) HMBC and (b) HMQC spectra of (R)-8 (5  $\mu$ M) with silver(I) triflate (1.0 equiv.).

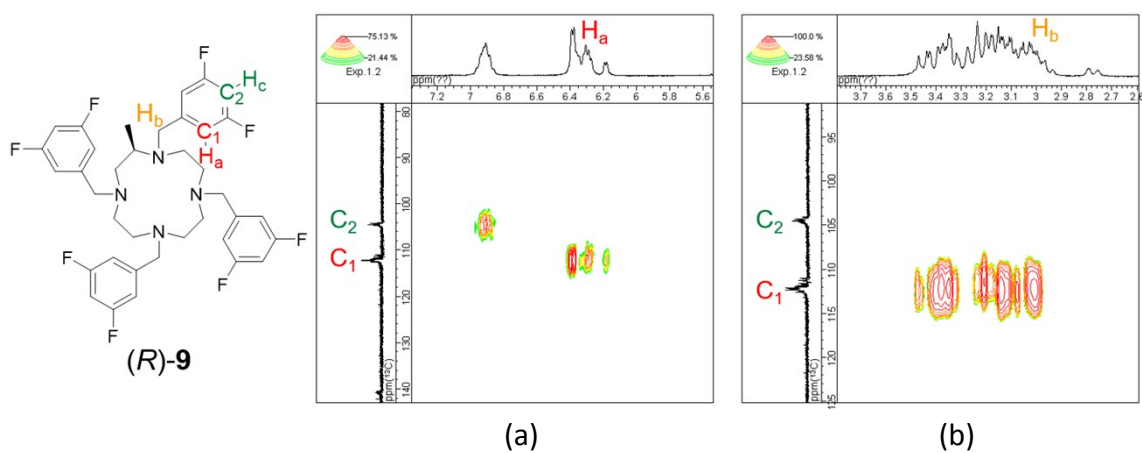


**Fig. S23** (a) HMBC and (b) HMQC spectra of (*R*)-**9** (5  $\mu$ M) with silver(I) triflate (1.0 equiv.).

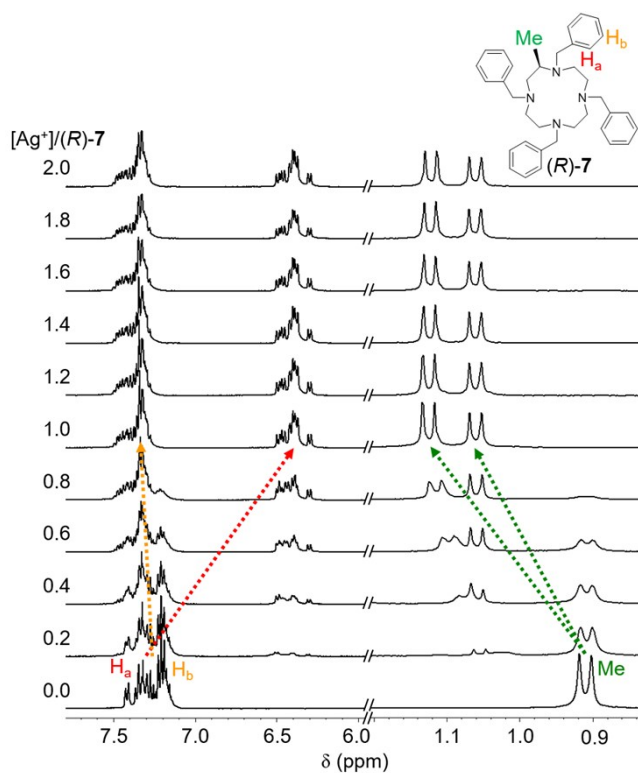


**Fig. S24** Silver(I)-induced  $^1\text{H}$  NMR spectral changes of (*R*)-**7** (5  $\mu$ M) in  $\text{CD}_2\text{Cl}_2/\text{CD}_3\text{OD}$  (1:1). When  $\text{Ag}^+$  was added to (*R*)-**7**, the  $\text{H}_a$  protons shifted to high field *ca.* by 0.90 ppm.

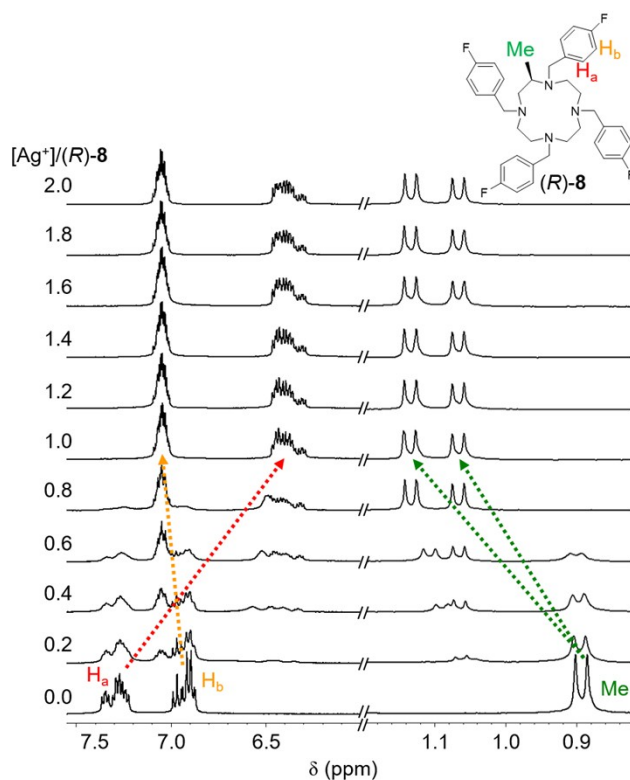


**Fig. S25** Silver(I)-induced  $^1\text{H}$  NMR spectral changes of (R)-8 (5  $\mu\text{M}$ ) in  $\text{CD}_2\text{Cl}_2/\text{CD}_3\text{OD}$  (1:1). When  $\text{Ag}^+$  was added to (R)-8, the  $\text{H}_a$  protons shifted to high field *ca.* by 0.91 ppm.

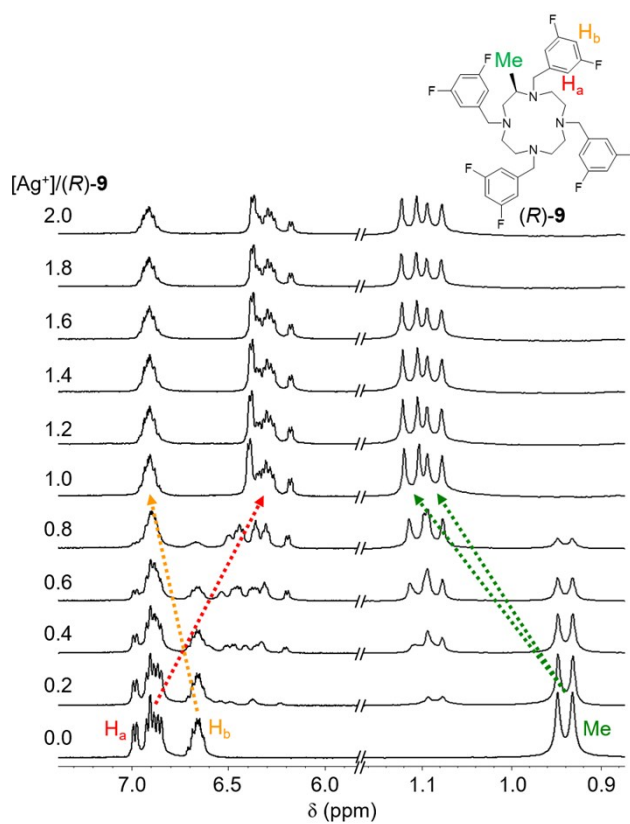


**Fig. S26** Silver(I)-induced  $^1\text{H}$  NMR spectral changes of (R)-9 (5  $\mu\text{M}$ ) in  $\text{CD}_2\text{Cl}_2/\text{CD}_3\text{OD}$  (1:1). When  $\text{Ag}^+$  was added to (R)-9, the  $\text{H}_a$  protons shifted to high field *ca.* by 0.62 ppm.

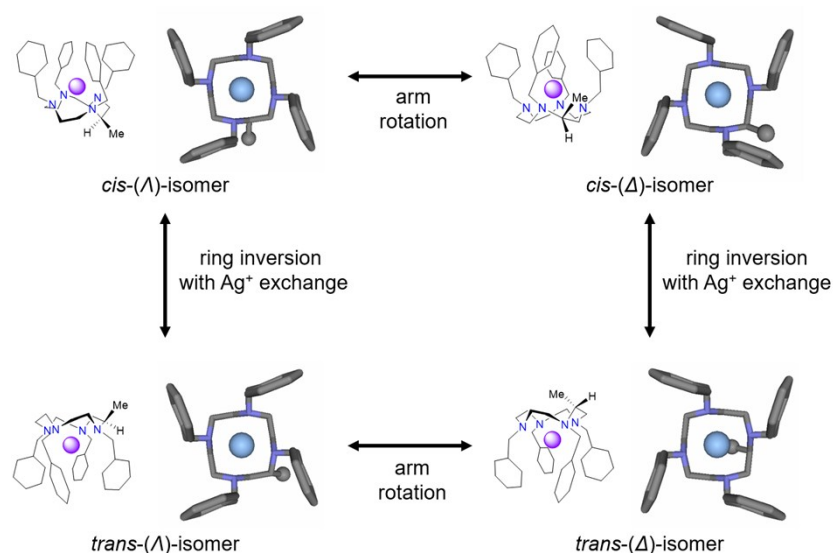


**Fig. S27** Four isomers of Ag<sup>+</sup> complexes with a chiral tetra-armed cyclen (the direction of rotation of four side-arms is denoted by  $\Lambda$  and  $\Delta$ , and the relative position of methyl group and the four aromatic rings related to the cycle of the cyclen is denoted by *cis* and *trans*).

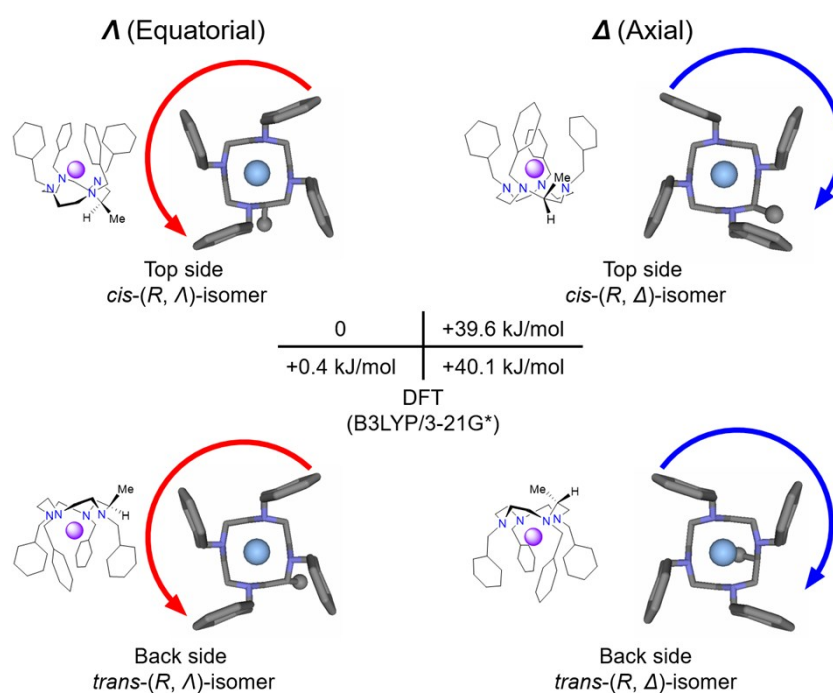


**Fig. S28** Molecular modeling calculation of Ag<sup>+</sup> complex of (*R*)-7.

**Table S1** Molecular modeling calculation of (*R*)-7-Ag<sup>+</sup> complex

	$\Lambda(\delta)$	$\Lambda(\lambda)$	$\Delta(\delta)$	$\Delta(\lambda)$
E (kJ/mol)	-4281918.808	-4281918.715	-4281909.341	-4281909.222
Relative energy (kJ/mol)*	0	+0.4	+39.6	+40.1
Ratio of formation	1	0.9	$1.47 \times 10^{-7}$	$1.14 \times 10^{-7}$

\*For better comparison the energies are relative to the  $\Lambda 1$  conformer of the lowest energy.

**Table S2** Molar ellipticity and  $\epsilon$  of the  $\text{Ag}^+$  complexes with chiral cyclens and minimum of potential energy, and dipole moments of substituted benzenes

	Molar ellipticity at 222 nm	$\epsilon$ at 222 nm		Minimum of potential energy (kJ/mol, B3LYP/6-31G*)	Dipole moment (D)
6	19600	27400	toluene	-94.5	0.32
7	6500	10600	benzene	-89.3	0
8	5000	11300	4-fluorobenzene	-79.0	1.36
9	9100	10100	1,3-difluorobenzene	-65.2	1.35

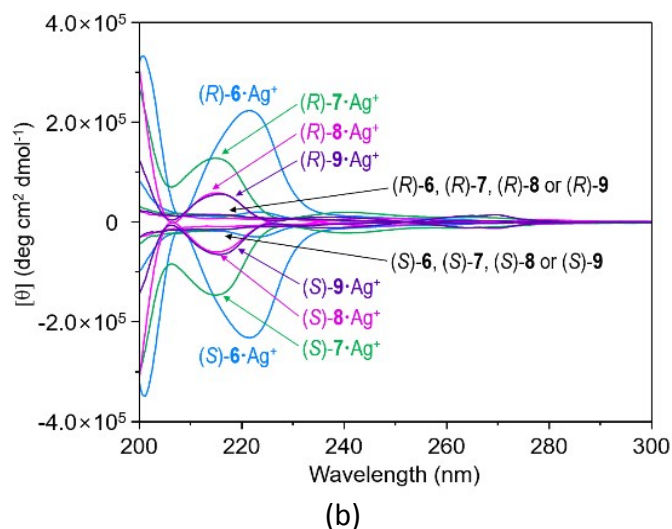
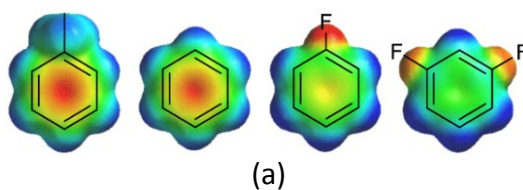


**Fig. S29** (a) Electrostatic potential maps of toluene, benzene, 4-fluoromethylbenzene and 1,3-difluoro-4-methylbenzene. (b) Comparison of the CD spectra of each ligand with 1 equiv. of silver(I) in  $\text{CHCl}_3:\text{CH}_3\text{OH}$  (1:19).



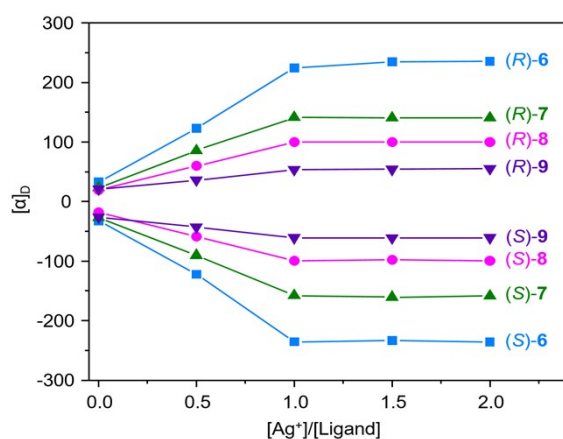


**Fig. S30** Ag<sup>+</sup>-induced change in optical rotation titration of each ligand with Ag<sup>+</sup> in CHCl<sub>3</sub>:CH<sub>3</sub>OH (1:19). Ag<sup>+</sup>-induced optical rotation ( $[\alpha]_D$ ) changes were carried out using (*R*)- and (*S*)-form **6–9**. As the stepwise addition of Ag<sup>+</sup>,  $[\alpha]_D$  values gradually increased between 0 and 1.0 equiv. of silver(I). An inflection points were observed at 1.0 (= [Ag<sup>+</sup>]/[ligand]), showing a 1:1 complexation.

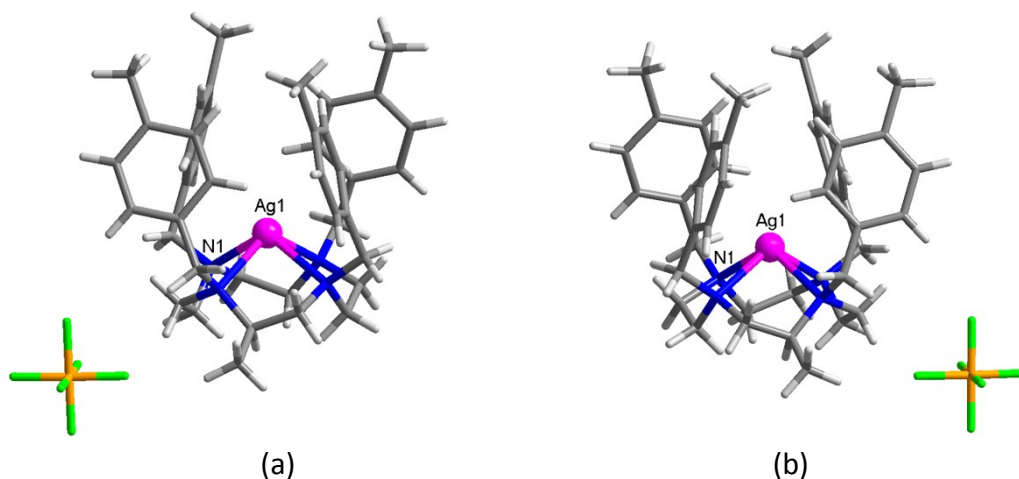


**Fig. S31** Crystal structures of (a) (*R*)-**6** and (b) (*S*)-**6** with AgPF<sub>6</sub>.

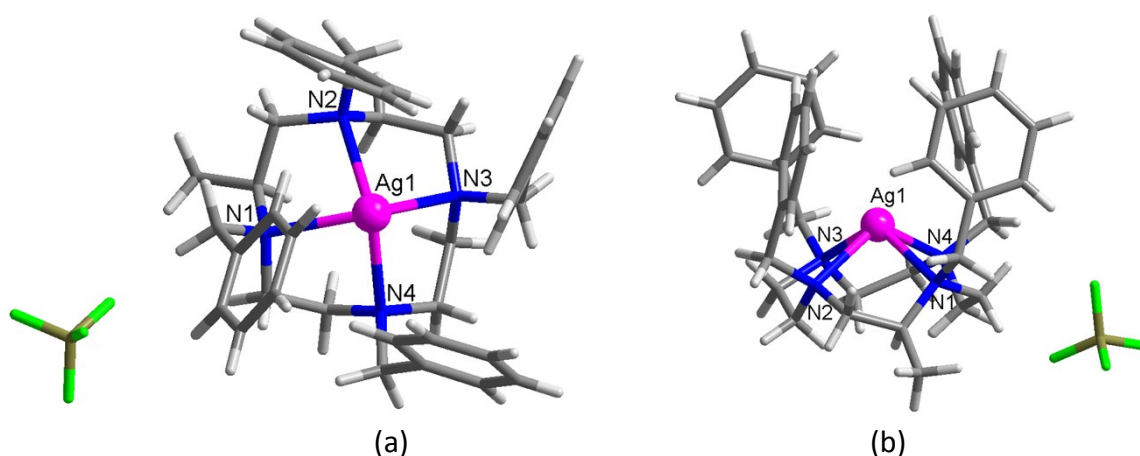


**Fig. S32** Crystal structure of (*S*)-**7** with AgBF<sub>4</sub>: (a) top view and (b) general view.

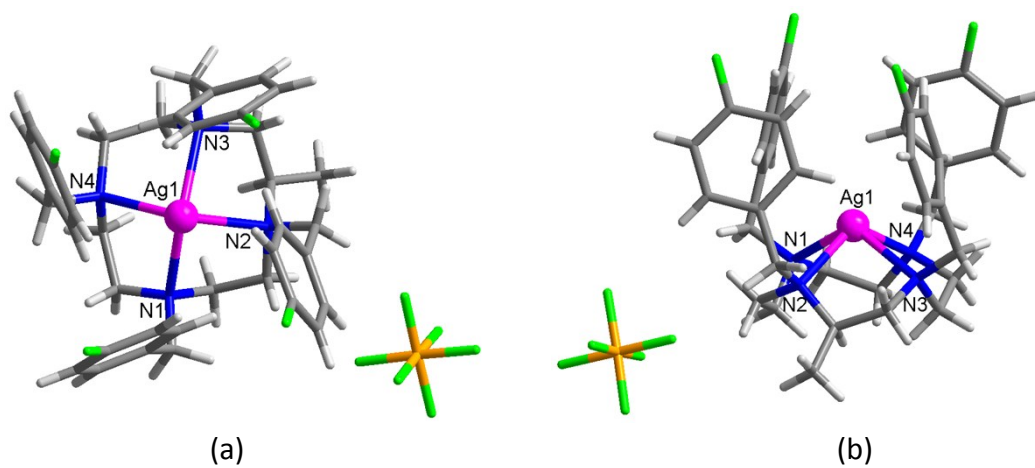


**Fig. S33** Crystal structure of (*R*)-**8** with  $\text{AgPF}_6$ : (a) top view and (b) general view.

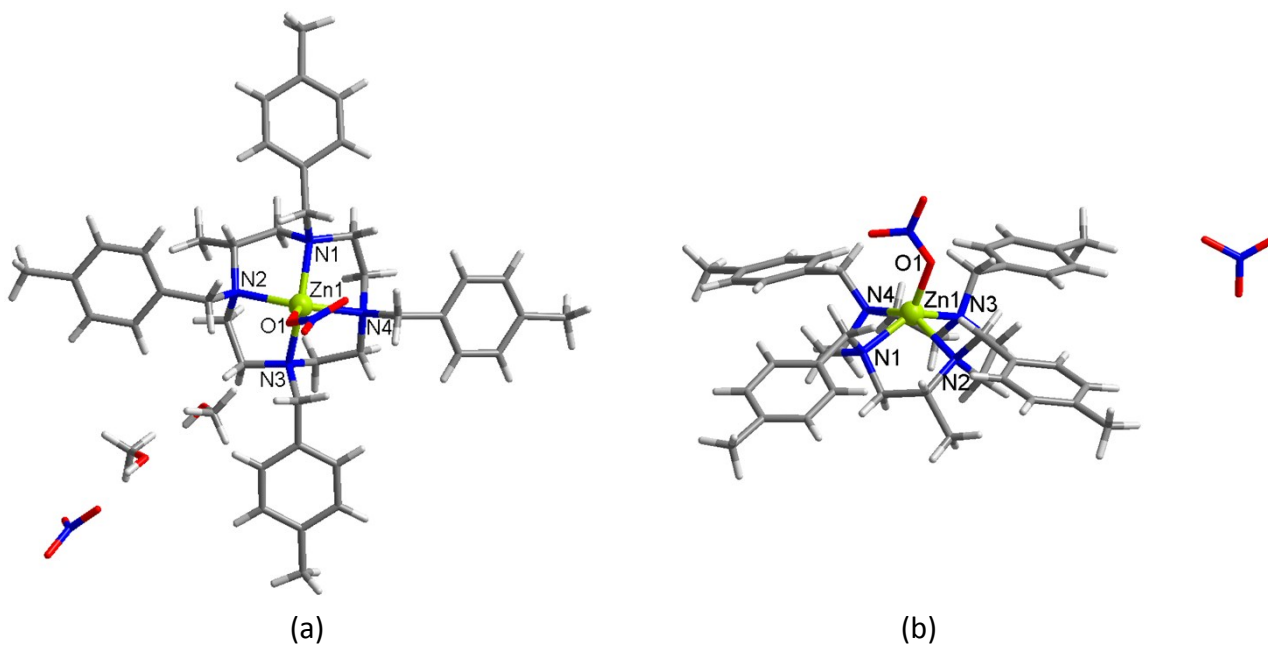


**Fig. S34** Crystal structure of (*R*)-**6** with  $\text{Zn}(\text{NO}_3)_2$ : (a) top view and (b) side view.

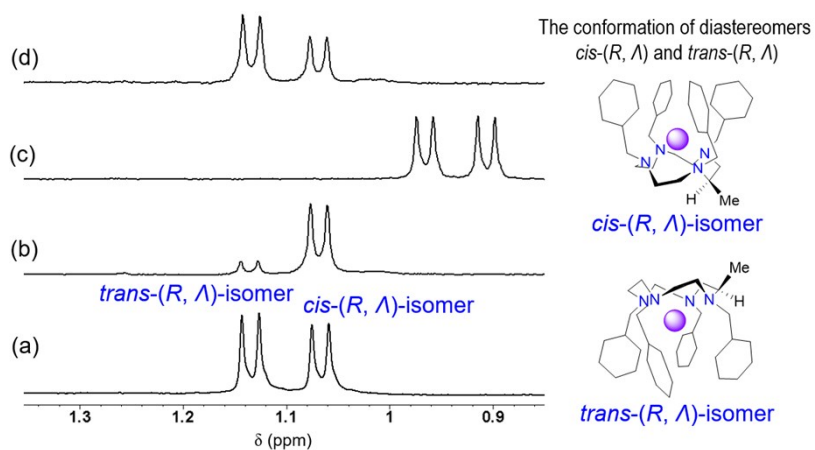


**Fig. S35** Methyl proton signals in the  $\text{Ag}^+/((R)\text{-8})$  system: (a) titration experiment ( $[\text{Ag}^+]/[(R)\text{-8}] = 1.0$ ) in  $\text{CD}_3\text{OD}/\text{CD}_2\text{Cl}_2$ , (b) single crystals dissolved in  $\text{CD}_3\text{OD}/\text{CD}_2\text{Cl}_2$ , (c) single crystals dissolved in  $\text{CD}_3\text{CN}$ , and (d) the solvent in (c) was changed to  $\text{CD}_3\text{OD}/\text{CD}_2\text{Cl}_2$ .

## X-ray crystallographic analysis.

All data were collected on a Bruker SMART APEX II ULTRA diffractometer equipped with graphite monochromated Mo  $K_{\alpha}$  radiation ( $\lambda = 0.71073 \text{ \AA}$ ) generated by a rotating anode. The cell parameters for the compounds were obtained from a least-squares refinement of the spot. Data collection, data reduction, and semi-empirical absorption correction were carried out using the software package of APEX2.<sup>4</sup> All of the calculations for the structure determination were carried out using the SHELXTL package.<sup>5</sup> In all cases, nonhydrogen atoms were refined anisotropically and hydrogen atoms were placed in idealized positions and refined isotropically in a riding manner along with their respective parent atoms. For the refinement of disordered atoms in (S)-7-AgBF<sub>4</sub> complex, the commands (ISOR, SADI, SIMU, etc.) have been used. Relevant crystal data collection and refinement data for the crystal structures are summarized in Table S3. CCDC 1975401 ((R)-6-AgPF<sub>6</sub>), 1975402 ((S)-6-AgPF<sub>6</sub>), 1975403 ((S)-7-AgBF<sub>4</sub>), 1975404 ((R)-8-AgPF<sub>6</sub>) and 1975405 ((R)-6-Zn(NO<sub>3</sub>)<sub>2</sub>) contain the supplementary crystallographic data for this paper. These data can be obtained free of charge from The Cambridge Crystallographic Data Centre via [www.ccdc.cam.ac.uk/data\\_request/cif](http://www.ccdc.cam.ac.uk/data_request/cif).

**Table S3** Crystal and experimental data

	(R)-6-AgPF <sub>6</sub>	(S)-6-AgPF <sub>6</sub>	(S)-7-AgBF <sub>4</sub>	(R)-8-AgPF <sub>6</sub>	(R)-6-Zn(NO <sub>3</sub> ) <sub>2</sub>
Formula	C <sub>41</sub> H <sub>54</sub> Ag <sub>1</sub> N <sub>4</sub> P <sub>1</sub> F <sub>6</sub>	C <sub>41</sub> H <sub>54</sub> Ag <sub>1</sub> N <sub>4</sub> P <sub>1</sub> F <sub>6</sub>	C <sub>37</sub> H <sub>46</sub> Ag <sub>1</sub> N <sub>4</sub> B <sub>1</sub> F <sub>4</sub>	C <sub>37</sub> H <sub>42</sub> Ag <sub>1</sub> N <sub>4</sub> P <sub>1</sub> F <sub>6</sub>	C <sub>43</sub> H <sub>62</sub> Zn <sub>1</sub> N <sub>6</sub> O <sub>8</sub>
Formula weight	855.72	855.72	741.46	871.58	856.35
Temperature	120(2)	120(2)	100(2)	90(2)	120(2)
Crystal system	Tetragonal	Tetragonal	Monoclinic	Orthorhombic	Monoclinic
Space group	<i>I</i> 4	<i>I</i> 4	<i>C</i> 2	<i>C</i> 222 <sub>1</sub>	<i>P</i> 2 <sub>1</sub>
<i>Z</i>	2	2	4	8	2
<i>a</i> (Å)	9.6472(15)	9.614(4)	13.8399(17)	13.8896(12)	8.7797(7)
<i>b</i> (Å)	9.6472(15)	9.614(4)	13.5554(16)	14.0055(12)	19.0092(15)
<i>c</i> (Å)	21.411(3)	21.337(8)	18.233(2)	37.666(3)	12.9597(10)
$\alpha$ (°)	90	90	90	90	90
$\beta$ (°)	90	90	100.627(2)	90	90.5449(16)
$\gamma$ (°)	90	90	90	90	90
<i>V</i> (Å <sup>3</sup> )	1992.7(7)	1972.2(17)	3361.9(7)	7327.3(11)	2162.8(3)
<i>D</i> <sub>calc</sub> (g/cm <sup>3</sup> )	1.426	1.441	1.465	1.580	1.315
2 $\theta$ <sub>max</sub> (°)	52.00	52.00	52.00	52.00	52.00
<i>R</i> <sub>1</sub> , <i>wR</i> <sub>2</sub> [ <i>I</i> > 2 $\sigma$ ( <i>I</i> )]	0.0279, 0.0595	0.0440, 0.1141	0.0600, 0.1743	0.0293, 0.0812	0.0555, 0.1182
<i>R</i> <sub>1</sub> , <i>wR</i> <sub>2</sub> [all data]	0.0292, 0.0599	0.0451, 0.1151	0.0617, 0.1781	0.0296, 0.0829	0.0965, 0.1404
Goodness-of-fit on <i>F</i> <sup>2</sup>	1.048	1.020	1.050	1.047	1.012
Flack parameter	-0.016(18)	-0.02(2)	0.04(4)	0.017(5)	0.08(3)
No. of reflection used [>2 $\sigma$ ( <i>I</i> )]	1794 [ <i>R</i> <sub>int</sub> = 0.0334]	1915 [ <i>R</i> <sub>int</sub> = 0.0404]	5609 [ <i>R</i> <sub>int</sub> = 0.0591]	7194 [ <i>R</i> <sub>int</sub> = 0.0184]	7643 [ <i>R</i> <sub>int</sub> = 0.0552]
Refinement	full-matrix	full-matrix	full-matrix	full-matrix	full-matrix

**Table S4** Selected bond lengths (Å) and bond angles (°) for (*R*)-**6**-AgPF<sub>6</sub>

Ag1-N1	2.467(4)		
N1-Ag1-N1A	76.3(1)	N1-Ag1-N1B	121.8(2)

Symmetry operations: (A)  $-x+2, y, z$  (B)  $-x+2, y+2, z$

**Table S5** Selected bond lengths (Å) and bond angles (°) for (*S*)-**6**-AgPF<sub>6</sub>

Ag1-N1	2.463(7)		
N1-Ag1-N1A	76.5(2)	N1-Ag1-N1B	122.2(3)

Symmetry operations: (A)  $-x+1, y-1, z$  (B)  $x+1, -y+1, z$

**Table S6** Selected bond lengths (Å) and bond angles (°) for (*S*)-**7**-AgBF<sub>4</sub>

Ag1-N1	2.468(9)	Ag1-N2	2.486(8)
Ag1-N3	2.450(9)	Ag1-N4	2.465(9)
N1-Ag1-N2	76.7(3)	N1-Ag1-N3	123.3(3)
N1-Ag1-N4	77.3(3)	N2-Ag1-N3	77.2(3)
N2-Ag1-N4	123.3(3)	N3-Ag1-N4	76.6(3)

**Table S7** Selected bond lengths (Å) and bond angles (°) for (*R*)-**8**-AgPF<sub>6</sub>

Ag1-N1	2.475(4)	Ag1-N2	2.449(4)
Ag1-N3	2.460(4)	Ag1-N4	2.446(4)
N1-Ag1-N2	77.1(1)	N1-Ag1-N3	123.5(1)
N1-Ag1-N4	76.8(1)	N2-Ag1-N3	77.0(1)
N2-Ag1-N4	123.6(1)	N3-Ag1-N4	77.5(1)

**Table S8** Selected bond lengths (Å) and bond angles (°) for (*R*)-**6**-Zn(NO<sub>3</sub>)<sub>2</sub>

Zn1-N1	2.116(8)	Zn1-N2	2.184(8)
Zn1-N3	2.152(8)	Zn1-N4	2.200(8)
Zn1-O1	1.959(5)		
N1-Zn1-N2	83.6(3)	N1-Zn1-N3	139.1(3)
N1-Zn1-N4	83.9(3)	N2-Zn1-N3	82.6(3)
N2-Zn1-N4	139.8(3)	N3-Zn1-N4	82.3(3)
N1-Zn1-O1	118.4(3)	N2-Zn1-O1	96.9(3)
N3-Zn1-O1	101.4(3)	N4-Zn1-O1	122.5(3)

## References

1. P. Gans, A. Sabatini and A. Vacca, *Talanta*, 1996, **43**, 1739–1753.
2. S. S. Insaf and D. T. Witiak, *Tetrahedron*, 2000, **56**, 2359–2367.
3. Q. Yuan, P. Xue, M. Fang, E. Fu and C. Wu, *Synthetic Commun.*, 2003, **33**, 1911–1916.
4. *APEX2 Version 2009.1-0 Data collection and Processing Software*; Bruker AXS Inc.: Madison, Wisconsin, U.S.A., 2008.
5. G. M. Sheldrick, Crystal structure refinement with SHELXL. *Acta Cryst.* 2015, **C71**, 3–8.